

# Block Level Image Fusion using Discrete Wavelet Transform

Research Thesis



Developed By:

Muhammad Hassan Arif

301-FAS/MSCS/F06

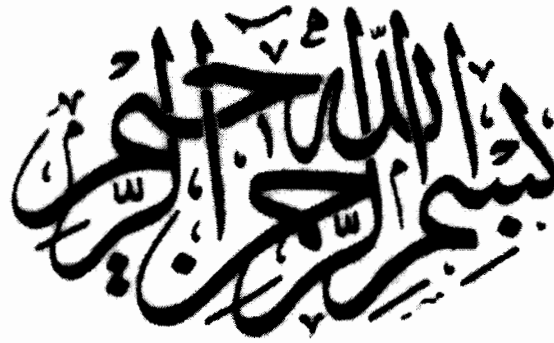
Supervised By:

Syed Muhammad Saqlain

Assistant Professor

Department of Computer Science  
Faculty of Basic and Applied Sciences  
International Islamic University Islamabad  
(2010)





**In The Name Of ALLAH, The Most Beneficial, The Most Merciful.**

**A dissertation submitted to the  
Department of Computer Science,  
International Islamic University, Islamabad  
As a partial fulfillment of the degree of  
MS Computer Science**

**Dedicated to My Great Uncle, Ahmad Hassan Raz  
Who Taught me How to Talk Allah.  
Who guided me in the way of Searching the Ultimate Truth.**

## Declaration

I hereby declare that this thesis report, neither as a whole nor as a part there of has been copied out from any source. If any part of this report is proved to be copied out or found to be reported. I shall stand by the consequences. No portion of the work presented in this report has been submitted in support of any application for any other degree or qualification of this or any other university or institute of learning.

Muhammad Hassan Arif

301-FAS/MSCS/F06

## Acknowledgement

All praise to Almighty Allah, the most merciful and compassionate, Who enabled me to complete this thesis.

I express my gratitude to my kind supervisor Syed Muhammad Saqlain who kept my morale high by his suggestions and appreciation. Without his precious guidance and help we could never be able to develop this software. I would like to express my gratitude to all of my teachers for their moral support and guidance.

I would like to acknowledge the support of my family members. I would like to admit that I owe all my achievements to my truly, sincere and most loving parents, brothers and sisters, and specially my wife and my children who spared me and keep me free to complete this tedious job.

And last but not the least; I would like to acknowledge the support of all my friends, especially Muhammad Iqal, who guided me and helped me throughout this thesis.

Muhammad Hassan Arif

### **Abstract**

The objective of image fusion is to generate a resultant fused image from a set of input images (of the same scene) which describes the scene better than any single input image with respect to some relevant properties. The fused image is obtained by extracting all the useful information from the source images while not introducing artifacts or inconsistencies which will distract human observers or the following machine processing. When a camera is to catch several objects that are in different distances away from it, the camera could not be focused on these objects simultaneously to get a clear image in any way. However, the camera can be focused on each object individually to get a clear image of it. To get a clear image containing all objects, the usual method is image fusion, which has been widely applied in some fields such as machine vision, digital camera and object recognition. For this purpose a new image fusion technique that is actually integration of multi-scale wavelet transform, gradient and mathematical morphology schemes, has been proposed. The proposed scheme uses adaptive block size. Different algorithms are devised using multilevel blocks of different sizes.

Muhammad Hassan Arif

301-FAS/MSCS/F06

---

## Table of Contents

|         |  |    |
|---------|--|----|
| 1       | INTRODUCTION .....   | 14 |
| 1.1     | Definitions and terminologies .....  | 14 |
| 1.1.1   | Image Fusion.....  | 14 |
| 1.1.1.1 | Advantages of Image Fusion .....   | 15 |
| 1.1.1.2 | Uses of Image Fusion .....   | 16 |
| 1.1.2   | Discrete Wavelet Transform (DWT) .....   | 17 |
| 1.1.3   | Image Registration .....   | 18 |
| 1.1.4   | Edge Detector.....   | 18 |
| 1.2     | Scope .....  | 19 |
| 1.3     | Tool .....   | 19 |
| 1.4     | Thesis outline .....   | 20 |
| 2       | LITERATURE REVIEW .....  | 21 |
| 2.1     | A Wavelet Based Algorithm for Multi-Focus Micro-Image Fusion.....  | 21 |
| 2.2     | Multi-Focus Image Fusion by Establishing Focal Connectivity .....  | 22 |
| 2.3     | Image Fusion Based On Addition of Wavelet Coefficients .....   | 23 |
| 2.4     | Image Fusion Based On Wavelet Transform .....  | 24 |
| 2.5     | Multifocus Image Fusion using Spatial Features and Support Vector Machine  | 25 |
| 2.6     | A Novel Support Vector Machine-Based Multifocus Image Fusion Algorithm   | 26 |
| 2.7     | The Wavelet-based Contourlet Transform for Image Fusion .....  | 27 |
| 2.8     | A Multifocus Image Fusion Based on Wavelet and Region Detection.....   | 28 |
| 2.9     | Image Fusion Algorithm Based on Neighbors and Cousins Information in<br>Nonsampled Contourlet Transform Domain ..... | 29 |
| 3       | Proposed Solution .....  | 31 |



---

|         |   |    |
|---------|---|----|
| 3.1     | Problem Statement .....   | 31 |
| 3.2     | Proposed Solution .....   | 32 |
| 3.2.1   | Proposed Block Level Multi-Focus Image Fusion Algorithms .....    | 32 |
| 3.2.1.1 | Fusion using Single Level Blocks .....                            | 36 |
| 3.2.1.2 | Fusion using Two Level Blocks .....                               | 38 |
| 3.2.1.3 | Fusion using Three Level Blocks .....                             | 40 |
| 3.2.1.4 | Fusion using Three Level Blocks and Mathematical Morphology ..... | 42 |
| 4       | Implementation Detail .....                                       | 44 |
| 4.1     | Acquiring Image.....  | 44 |
| 4.2     | Blocking and Discrete Wavelet Transform.....                      | 46 |
| 4.3     | Maxima of Wavelet Coefficients using Compass Edge Detectors ..... | 46 |
| 4.4     | Enhancement of Maxima .....                                       | 47 |
| 4.5     | Construction of Binary Decision Map .....                         | 47 |
| 4.6     | Morphological Operations.....                                     | 47 |
| 4.7     | Construction of the fused image.....                              | 48 |
| 4.8     | The Simulation .....  | 48 |
| 5       | Results and Comparisons.....                                      | 53 |
| 5.1     | Image Quality Evaluation Matrices.....                            | 53 |
| 5.1.1   | Peak Signal to Noise Ratio (PSNR).....                            | 53 |
| 5.1.2   | Root Mean Square Error (RMSE).....                                | 53 |
| 5.1.3   | Spatial Frequency (SF) .....                                      | 53 |
| 5.2     | Edge Detectors Comparison.....                                    | 54 |
| 5.3     | Comparisons of Fused Image with Source Images .....               | 56 |
| 5.4     | Comparison of Proposed Approaches with Existing Methods.....      | 57 |

---

|     |                                  |    |
|-----|----------------------------------|----|
| 6   | CONCLUSION AND FUTURE WORK ..... | 64 |
| 6.1 | Conclusion.....                  | 64 |
| 6.2 | Future Work .....                | 65 |
| 7   | References.....                  | 66 |

## Table of Figures

|   |    |
|---|----|
| Figure 1-1 : Source and Fused Images.....   | 15 |
| Figure 1-2 : 3-Level Decomposition of 2-D DWT .....   | 17 |
| Figure 1-3: Compass Edge Detectors .....  | 19 |
| Figure 2-1: Image Fusion based on Addition of wavelet coefficients .....                                  | 23 |
| Figure 2-2: The image fusion framework based on WBCT.....   | 27 |
| Figure 2-3: Image fusion using Nonsubsampled contourlet Transform .....                                   | 30 |
| Figure 3-1: Block clarity algorithm .....   | 34 |
| Figure 3-2: Boundary blocks fusion algorithm .....  | 35 |
| Figure 3-3: Fusion using Single level blocks.....   | 37 |
| Figure 3-4: Fusion using Two Level Blocks.....  | 39 |
| Figure 3-5: Fusion using Three Level Blocks.....  | 41 |
| Figure 3-6: Fusion using Three Level Blocks and Mathematical Morphology .....                             | 43 |
| Figure 4-1: Original Barbara test image (512 x 512).....  | 44 |
| Figure 4-2: Multifocused Sources Images of Barbara's .....  | 45 |
| Figure 4-3: Prewitt Edge Detector .....   | 47 |
| Figure 4-4: The resulting fused image .....   | 48 |
| Figure 4-5: Screen shot of start window in MATLAB .....   | 49 |
| Figure 4-6: Fusion result against left-right defocused Lena image using 16 by 16 blocks<br>.....          | 50 |
| Figure 4-7: Fusion result against upper-lower defocused Lena image using 8 by 8 blocks<br>.....           | 51 |
| Figure 4-8: Result against inner-outer defocused Barbara image using 2-level blocks<br>fusion method..... | 51 |
| Figure 4-9: Result against upper-lower defocused Peppers image using 3-level blocks<br>fusion method..... | 52 |
| Figure 4-10: Result against left-right defocused Gold-Hill image using morphological<br>method.....       | 52 |
| Figure 5-1: Graphical Comparison of RMSE .....  | 62 |
| Figure 5-2: Graphical Comparison of PSNR.....   | 62 |

---

Figure 5-3: Graphical Comparison of SF..... 63

## Table of Tables

|  |    |
|--|----|
| Table 5-1: Fusion results using Robinson edge detector .....           | 54 |
| Table 5-2: Fusion results using Sobel edge detector.....               | 54 |
| Table 5-3: Fusion results using Kirsch edge detector .....             | 55 |
| Table 5-4: Fusion results using Prewitt edge detector .....            | 55 |
| Table 5-5: Comparison with Input Images of Lena .....                  | 56 |
| Table 5-6: Comparison with Input Images of Barbara .....               | 56 |
| Table 5-7: Comparison with Input Images of Peppers .....               | 57 |
| Table 5-8: Comparison with Input Images of Gold Hill.....              | 57 |
| Table 5-9: Image Fusion Methods' Comparisons for Lena Image .....      | 58 |
| Table 5-10: Image Fusion Methods' Comparisons for Barbara Image .....  | 59 |
| Table 5-11: Image Fusion Methods' Comparisons for Peppers Image .....  | 60 |
| Table 5-12: Image Fusion Methods' Comparisons for Gold-Hill Image..... | 61 |

# 1 INTRODUCTION

Image fusion is a new and emerging research technique in this decade. There can be multiple images of the same scene captured from different cameras providing useful information about the scene. None of these images fully describe the scene, each image have some information so all these images should be fused to produce an image which fully describe the scene and contains more information than any of the single input image. For examples,

1. Optical lenses of microscopic devices has problem of limited depth-of-focus, it is often not possible to get an image that contains all relevant objects “in focus”. To achieve all objects “in focus”, a fusion process is required so that all focused objects are selected.
2. Two types of sensors are used in remote sensing, one for color information and one for detailed information. Three sensors are used to provide color information sensors covering the red, green and blue spectral wavelengths. These sensors have a low number of pixels (low spatial resolution) and the small objects and details (cars, small lines, etc.) are hidden. Such small objects and details can be observed with a different sensor (panchromatic), which have a high number of pixels (high spatial resolution) but without color information. With a fusion process a unique image can be achieved containing both high spatial resolution and color information.

## 1.1 Definitions and terminologies

This section introduces various terminologies and definitions incorporating image fusion process. These terms are image fusion, image registration, Wavelet Transform, and edge detectors.

### 1.1.1 Image Fusion

Image fusion can be defined as a merger of multiple source images, describing different parts of a scene, in order to produce an image which is more robust, sharply focused, geometrically more correct and have less artifacts. The resultant image is more suitable

for human visualization and machine observation. It can also be used for further image-processing tasks like pattern recognition, face recognition and feature extraction.

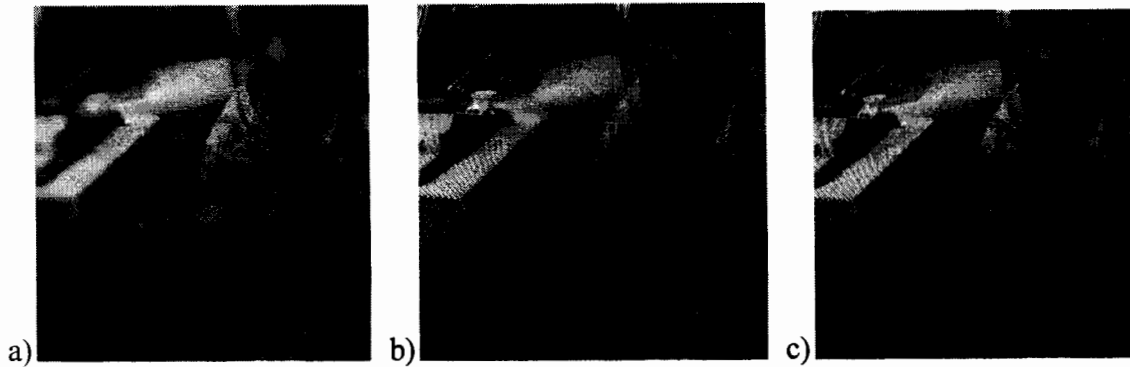


**Figure 1-1 : Source and Fused Images**

**a) Input Image1 b) Input Image2 c) Fused Image**

### **1.1.1.1 Advantages of Image Fusion**

Image fusion provides following advantages:

1. Faster acquisition of information (Simultaneous data acquisition by using multiple sensors)
2. Feature Vector with Higher Dimensionality (by evaluation of complementary information)
3. Cost-effective acquisition of information (Substitution of expensive special sensors with several low-cost sensors)
4. Extended range of operation: multiple sensors that operate under different operating conditions can be deployed to extend the effective range of operation. For example different sensors can be used for day/night operation.
5. Extended spatial and temporal coverage: joint information from sensors that differ in spatial resolution can increase the spatial coverage. The same is true for the temporal dimension.
6. Reduced uncertainty: joint information from multiple sensors can reduce the uncertainty associated with the sensing or decision process.

7. Increased reliability: the fusion of multiple measurements can reduce noise and therefore improve the reliability of the measured quantity.
8. Robust system performance: redundancy in multiple measurements can help in systems robustness. In case one or more sensors fail or the performance of a particular sensor deteriorates, the system can depend on the other sensors.
9. Compact representation of information: fusion leads to compact representations. For example, in remote sensing, instead of storing imagery from several spectral bands, it is comparatively more efficient to store the fused information

### **1.1.1.2 Uses of Image Fusion**

#### **a) Intelligent Robots**

- Require motion control, based on feedback from the environment from visual, tactile, force/torque, and other types of sensors
- Stereo camera fusion
- Intelligent viewing control
- Automatic target recognition and tracking

#### **b) Medical Imaging**

- Fusing X-ray computed tomography (CT) and magnetic resonance (MR) images
- Computer assisted surgery
- Spatial registration of 3-D surface

#### **c) Manufacturing**

- Electronic circuit and component inspection
- Product surface measurement and inspection
- Non-destructive material inspection
- Manufacture process monitoring
- Complex machine/device diagnostics
- Intelligent robots on assembly lines

#### **d) Military and Law Enforcement**

- Detection, tracking, identification of ocean (air, ground) target/event



- Concealed weapon detection
  - Battle-field monitoring
  - Night pilot guidance
- e) **Remote Sensing**
- Using various parts of the electro-magnetic spectrum
  - Sensors: from black-and-white aerial photography to multi-spectral active microwave space-borne imaging radar
  - Fusion techniques are classified into photographic method and numerical method

### 1.1.2 Discrete Wavelet Transform (DWT)

DWT is a method to analyze image. The discrete wavelet transform coefficients represent non-redundant information of image. The DWT can be decomposed to N level. At each level decomposition four frequency bands are produced. These bands represent approximation and detailed coefficients. The detailed coefficients further divided into horizontal, vertical and diagonal details. The approximation and detailed coefficients are also called Low-Low (LL), High-Low (HL), Low-High (LH) and High-High (HH). As shown in figure.

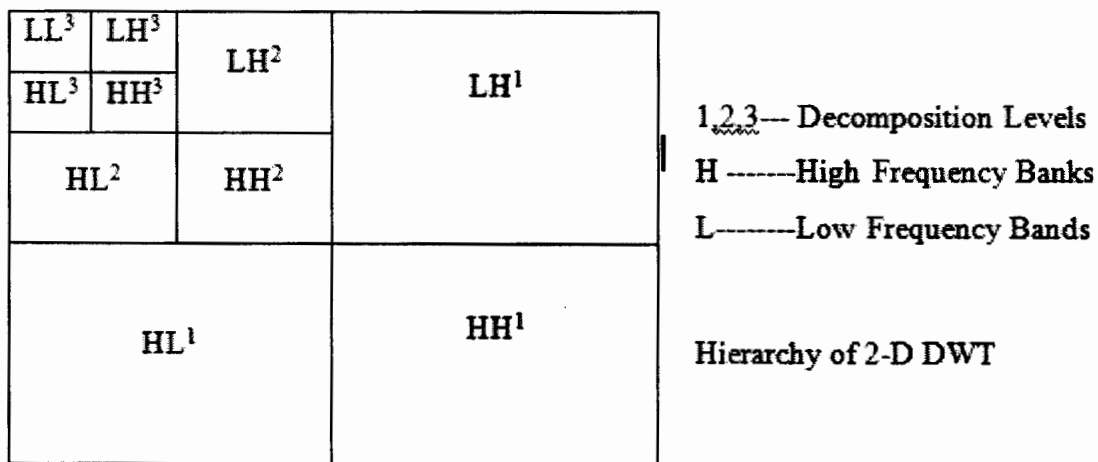


Figure 1-2 : 3-Level Decomposition of 2-D DWT

The figure represents 3 level decomposition of DWT. Approximation can be further subdivided to next level decomposition. It further subdivides the approximation to four

sub bands. It is recursive decomposition procedure.  $3N+1$  frequency bands are produced when DWT is decomposed to  $N$  levels.

### 1.1.3 Image Registration

There are very often some issues that have to be dealt with before the fusion can be performed. Most of the time, the input images are misaligned. Misalignment of image features is caused by several factors including the geometries of the sensors, different spatial positions of the sensors, different temporal capture rates of the sensors and the inherent misalignment of the sensing elements. Image registration techniques align the images by exploiting the similarities between the input images.

### 1.1.4 Edge Detector

Edge detectors facilitate in tracing sharply focused regions. In Compass Edge Detection technique differential gradient is computed to detect sharp edges in image. The Compass Edge Detectors estimates both local gradient and edge orientation, resulting in two output images. Compass edge detectors uses 8 convolution kernels, each represents edges in different direction starting from  $0^\circ$ , in jumps of  $45^\circ$ , up to  $315^\circ$ .

Various kernels like Robinson, Sobel, Kirsch and Prewitt can be used for this operation, shown in Figure 1.5. Only two kernels out of 8 are shown. The remaining 6 kernels are produced by rotating the coefficients circularly. Each of these kernels represents edges in different direction. These gradient operators handle more gradual transition and noisier images better.

|          | $0^\circ$   | $45^\circ$ |   |   |    |    |   |    |   |   |   |   |   |   |    |    |   |    |    |   |
|----------|---|------------|---|---|----|----|---|----|---|---|---|---|---|---|----|----|---|----|----|---|
| Robinson | <table border="1"> <tr><td>-1</td><td>1</td><td>1</td></tr> <tr><td>-1</td><td>-2</td><td>1</td></tr> <tr><td>-1</td><td>1</td><td>1</td></tr> </table> | -1         | 1 | 1 | -1 | -2 | 1 | -1 | 1 | 1 | <table border="1"> <tr><td>1</td><td>1</td><td>1</td></tr> <tr><td>-1</td><td>-2</td><td>1</td></tr> <tr><td>-1</td><td>-1</td><td>1</td></tr> </table> | 1 | 1 | 1 | -1 | -2 | 1 | -1 | -1 | 1 |
| -1       | 1   | 1          |   |   |    |    |   |    |   |   |   |   |   |   |    |    |   |    |    |   |
| -1       | -2  | 1          |   |   |    |    |   |    |   |   |   |   |   |   |    |    |   |    |    |   |
| -1       | 1   | 1          |   |   |    |    |   |    |   |   |   |   |   |   |    |    |   |    |    |   |
| 1        | 1   | 1          |   |   |    |    |   |    |   |   |   |   |   |   |    |    |   |    |    |   |
| -1       | -2  | 1          |   |   |    |    |   |    |   |   |   |   |   |   |    |    |   |    |    |   |
| -1       | -1  | 1          |   |   |    |    |   |    |   |   |   |   |   |   |    |    |   |    |    |   |
| Sobel    | <table border="1"> <tr><td>-1</td><td>0</td><td>1</td></tr> <tr><td>-2</td><td>0</td><td>2</td></tr> <tr><td>-1</td><td>0</td><td>1</td></tr> </table>  | -1         | 0 | 1 | -2 | 0  | 2 | -1 | 0 | 1 | <table border="1"> <tr><td>0</td><td>1</td><td>2</td></tr> <tr><td>-1</td><td>0</td><td>1</td></tr> <tr><td>-2</td><td>-1</td><td>0</td></tr> </table>  | 0 | 1 | 2 | -1 | 0  | 1 | -2 | -1 | 0 |
| -1       | 0   | 1          |   |   |    |    |   |    |   |   |   |   |   |   |    |    |   |    |    |   |
| -2       | 0   | 2          |   |   |    |    |   |    |   |   |   |   |   |   |    |    |   |    |    |   |
| -1       | 0   | 1          |   |   |    |    |   |    |   |   |   |   |   |   |    |    |   |    |    |   |
| 0        | 1   | 2          |   |   |    |    |   |    |   |   |   |   |   |   |    |    |   |    |    |   |
| -1       | 0   | 1          |   |   |    |    |   |    |   |   |   |   |   |   |    |    |   |    |    |   |
| -2       | -1  | 0          |   |   |    |    |   |    |   |   |   |   |   |   |    |    |   |    |    |   |

|         |  |    |    |   |    |   |   |    |    |   |  |    |   |   |    |   |   |    |    |    |
|---------|--|----|----|---|----|---|---|----|----|---|--|----|---|---|----|---|---|----|----|----|
| Kirsch  | <table border="1"><tr><td>-3</td><td>-3</td><td>5</td></tr><tr><td>-3</td><td>0</td><td>5</td></tr><tr><td>-3</td><td>-3</td><td>5</td></tr></table> | -3 | -3 | 5 | -3 | 0 | 5 | -3 | -3 | 5 | <table border="1"><tr><td>-3</td><td>5</td><td>5</td></tr><tr><td>-3</td><td>0</td><td>5</td></tr><tr><td>-3</td><td>-3</td><td>-3</td></tr></table> | -3 | 5 | 5 | -3 | 0 | 5 | -3 | -3 | -3 |
|         | -3   | -3 | 5  |   |    |   |   |    |    |   |  |    |   |   |    |   |   |    |    |    |
|         | -3   | 0  | 5  |   |    |   |   |    |    |   |  |    |   |   |    |   |   |    |    |    |
| -3      | -3   | 5  |    |   |    |   |   |    |    |   |  |    |   |   |    |   |   |    |    |    |
| -3      | 5  | 5  |    |   |    |   |   |    |    |   |  |    |   |   |    |   |   |    |    |    |
| -3      | 0  | 5  |    |   |    |   |   |    |    |   |  |    |   |   |    |   |   |    |    |    |
| -3      | -3   | -3 |    |   |    |   |   |    |    |   |  |    |   |   |    |   |   |    |    |    |
| Prewitt | <table border="1"><tr><td>-1</td><td>0</td><td>1</td></tr><tr><td>-1</td><td>0</td><td>1</td></tr><tr><td>-1</td><td>0</td><td>1</td></tr></table>   | -1 | 0  | 1 | -1 | 0 | 1 | -1 | 0  | 1 | <table border="1"><tr><td>0</td><td>1</td><td>1</td></tr><tr><td>-1</td><td>0</td><td>1</td></tr><tr><td>-1</td><td>-1</td><td>0</td></tr></table>   | 0  | 1 | 1 | -1 | 0 | 1 | -1 | -1 | 0  |
|         | -1   | 0  | 1  |   |    |   |   |    |    |   |  |    |   |   |    |   |   |    |    |    |
|         | -1   | 0  | 1  |   |    |   |   |    |    |   |  |    |   |   |    |   |   |    |    |    |
| -1      | 0  | 1  |    |   |    |   |   |    |    |   |  |    |   |   |    |   |   |    |    |    |
| 0       | 1  | 1  |    |   |    |   |   |    |    |   |  |    |   |   |    |   |   |    |    |    |
| -1      | 0  | 1  |    |   |    |   |   |    |    |   |  |    |   |   |    |   |   |    |    |    |
| -1      | -1   | 0  |    |   |    |   |   |    |    |   |  |    |   |   |    |   |   |    |    |    |

Figure 1-3: Compass Edge Detectors

## 1.2 Scope

Scope of this research is to devise a better technique of image fusion for multifocused microscopic images, having problem of depth of focus, using wavelet transform. It is supposed that images are already appropriately registered. The performance of the proposed technique will be compared with previous image fusion techniques using standard evaluation metrics to provide evidence of better performance of proposed approach. The results will be shown using standard images as data set.

## 1.3 Tool

The proposed approach is practically be implemented and tested using *MATLAB 7*. One of the reasons of selecting *MATLAB* in this research is because it fits perfectly in the necessities of an image processing research due to its inherent characteristics. In addition, *MATLAB 7* has Image Processing Toolbox which helps in performing different image processing tasks, including:

- ✓ Geometric operations
- ✓ Neighborhood and block operations
- ✓ Transforms
- ✓ Image analysis and enhancement
- ✓ Binary image operations
- ✓ Region of interest operations

However, this application has some limitations. Probably the most restricting is the computation time. A real time application should be computed in some other more time efficient language such as C/C++ or similar.

#### **1.4 Thesis outline**

Chapter 2 describes the literature review related to image fusion process. Then the next chapter presents the problem statement and proposed solution. Chapter 4 describes the implementation detail for the proposed approach and gives a view of simulation. Chapter 5 presents the experimental results on standard test images against the recommended quality metrics and show comparisons of the results achieved by proposed scheme with results obtained from previous fusion techniques. Chapter 6 narrates conclusion and future work.

## 2 LITERATURE REVIEW

Image fusion is a hot research topic in current era, due to its wide applications like computer vision, target detection, object recognition, robotics, medical imaging, military and law enforcement etc. Image fusion can be carried out in spatial as well as frequency domain. We have studied many research papers and few of them are as follow.

### 2.1 A Wavelet Based Algorithm for Multi-Focus Micro-Image Fusion.

Fusion can be done in spatial domain as well as in transformed domain. This paper discusses the comparison of fusion techniques in spatial and transform domain and then proposes an algorithm in transform domain. Two main spatial domain operations are “Tenengrad function based on Sobel Operator” and Sum Modified Laplacian Operator”. Spatial domain fusion algorithms:

- Produces better results with good imaging conditions but complex images lose internal detail and edge information.
- Produces blocking effects for largely out of focus or distinct source images
- Don't perform well with transparent micro-images.

The algorithm is:

- a. Take average of the approximate coefficients.
- b. For detailed coefficients, considering each pixel as center of a 3x3 or 5x5 window; compute sum of all the coefficients within the window.
- c. Select maximum detailed coefficient from the window having higher summation value.

The area based wavelet fusion algorithm produces better results visually. It produces images having smooth edges and without coalescent marks. But this method may produce thick edges and extra smoothing.

In this paper no objective evaluation of the results is done, only subjective evaluations are given. It would be better if the authors use some performance evaluation criteria to support their proposed algorithm.

## 2.2 Multi-Focus Image Fusion by Establishing Focal Connectivity

Multifocus image fusion methods can be classified in three categories.

- a. Selective Region Based Methods
- b. Multiscale Decomposition Based Methods
- c. Learning Based Methods

This paper works with selective region based methods and propose a new segmentation technique which depends on focal connectivity. A region which is focally connected can be defined as: “A region or a set of regions in an input image that fall on the same focal plane”. A focally connected region may not be connected physically or geometrically. There is no ringing effect and this method is intelligence and computationally time effective.

- a. Calculate sharpness map for each input image using gradient.
- b. Apply low pass filter to sharpness maps.
- c. Using these sharpness maps it segments each source image into different partitions based on focal connectivity.
- d. Union of such partitions forms the fused image.

If all the corresponding regions in source images are blurred then this method chooses the region that is least blur. This method is able to handle unseen data.

## 2.3 Image Fusion Based On Addition of Wavelet Coefficients

This paper proposes a new technique to merge Discrete Wavelet Transform coefficients of two remote sensing images. One image is high spatial resolution panchromatic image and other is multi-spectral image with color information. The proposed technique “Addition of Wavelet Coefficients” is as follows:

- Convert RGB multispectral image to HSV (Hue, Saturation and Value) using HSV transform.
- V component is normalized in two components, V is in the intervals [0,255] and V1 is in the interval [0,1].
- Decompose V, V1 and Panchromatic image using DWT.
- Merge approximation information: V1 approximation plus panchromatic approximation.
- Merge detail information: choose maximum coefficient between V’s detail and panchromatic detail.
- A new value component V’ is obtained by applying IDWT.
- Convert H, S and V’ to RGB using inverse HSV transform.

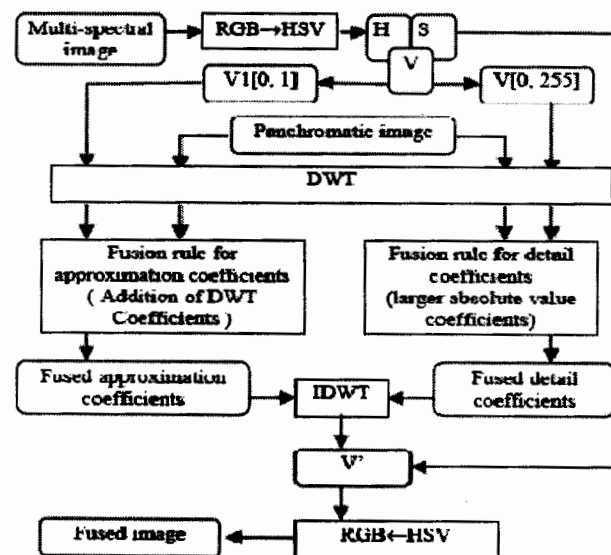


Figure 2-1: Image Fusion based on Addition of wavelet coefficients

An objective comparison is made with classical wavelet transformed based methods and results are found better.

## 2.4 Image Fusion Based On Wavelet Transform

Image fusion can be done on

- Pixel Level
- Feature Level
- Decision Level

The most common type in which comparison is done at individual pixels or among the pixels of a region in source images is pixel level. Featured based fusion uses the framework of region based fusion.

This paper proposes a technique base on pixel level fusion scheme using wavelet transform. The proposed technique calculates activity level. The proposed algorithm is as follows:

- a. Decompose the source image applying wavelet transform.
- b. Calculate average of the approximate coefficients.
- c. Compute activity level for detailed coefficients using the following equation.

$$saliency = \sum_{k=1}^{-j} |w(k)C^{(k)}(W_{2^j}f(n))|$$

Where

$w(k)$  is the weight of the maximum wavelet coefficients at different scales,  $C^{(k)}(W_{2^j}f(n))$  are the children of the coefficients  $W_{2^j}f(n)$ .

- d. The detailed coefficients with higher activity level values are selected for fused image.



- e. IDWT is applied to get fused image.

The proposed algorithm gives a new technique to calculate the activity level value, different fusion rules and fusion operators can use this activity level value.

## **2.5 Multifocus Image Fusion using Spatial Features and Support Vector Machine**

Transformed based fusion techniques perform satisfactorily but these techniques are not shift invariant. So in case of misregistration of the source images or slight object/camera movement, performance of decomposition based techniques degraded quickly.

This paper proposes a fusion technique in spatial domain using spatial features of image and a support vector machine (SVM) which solves the problem of shift invariance. The proposed approach is:

- a. Decompose the source images into blocks.
- b. Compute spatial features: spatial frequency (SF) and absolute central moments (ACM) of each block.
- c. Train an SVM to determine the clearer block based on SF and ACM.
- d. Select clearer blocks from the source images and fused to generate fused image.
- e. Majority filter is applied on the resultant image.

Source images are divided in blocks. It saves lots of computation and performs well. This technique provides better results than decomposition based techniques, if the images are misregistered.

In this paper no objective evaluation of the results is done, only subjective evaluations are given. It would be better if the authors use some performance evaluation criteria to support their proposed algorithm.

## 2.6 A Novel Support Vector Machine-Based Multifocus Image Fusion Algorithm

An algorithm with SVM and adaptive image block size is proposed for multifocus images. The proposed algorithm is:

- a. Decompose source images into blocks of size  $16 \times 16$ .
- b. For each block three features i.e., standard deviation, the DCT high frequency energy and the spatial frequency are selected to reflect its clarity.
- c. An SVM is trained to determine the clear blocks using the above mentioned clarity features. A binary matrix is created reflecting the clarity of blocks.
- d. Majority filter of size  $3 \times 3$  is applied on binary matrix.
- e. Decompose source images into blocks of size  $8 \times 8$ .
- f. Determine the boundary blocks from binary matrix.
- g. A new binary matrix for blocks of size  $8 \times 8$  is constructed:
  - i. Clarity of boundary blocks is determined using step c.
  - ii. Clarity decision of non boundary blocks is retained as it is in binary matrix for blocks of size  $16 \times 16$ .
- h. Apply majority filter of size  $3 \times 3$  on binary matrix.
- i. Determine the boundary blocks from new binary matrix:
  - i. Fuse the boundary blocks using DCT.
  - ii. Select the non boundary blocks from source images.

An SVM needs to be trained to incorporate the adaptive block size and to have full benefits of multi level blocks. As the large blocks have more information of edges and small image blocks have more detail.

## 2.7 The Wavelet-based Contourlet Transform for Image Fusion

A wavelet-based contourlet transform (WBCT) is used for image fusion in this paper.

The proposed scheme is given below:

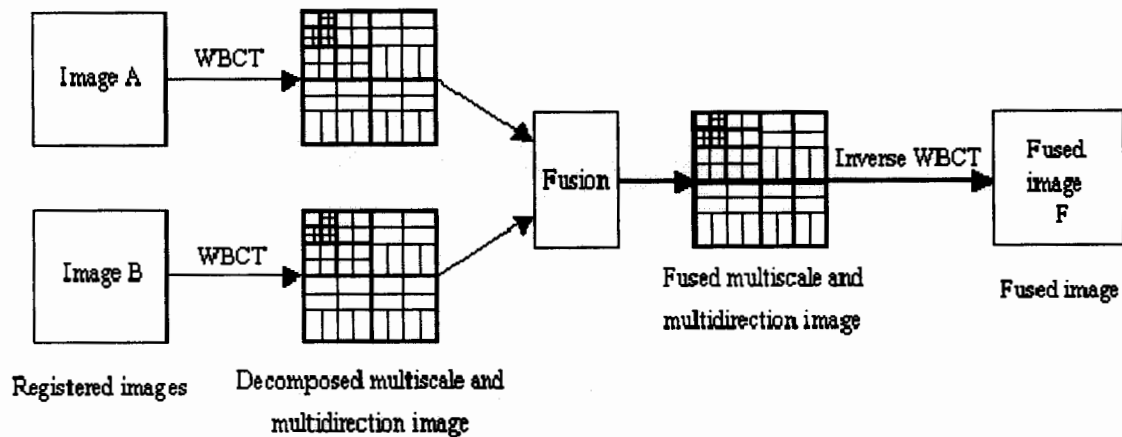


Figure 2-2: The image fusion framework based on WBCT

- a. Apply WBCT on registered source images.
- b. Get weighted average of low frequency coefficients.
- c. Calculate regional energy for each detailed coefficients.
- d. Select the coefficient with higher (than a certain threshold) energy than the corresponding coefficient. Otherwise get weighted average of the two coefficients.
- e. Apply inverse WBCT to get the resultant fused image.

Results of three other methods: Laplacian pyramid, Wavelet and Contourlet are compared with WBCT using four objective evaluation metrics; Mean Cross Entropy, Root Cross Entropy, Sharpness, and Entropy. The experimental results show that WBCT based fusion produces the best results.

## 2.8 A Multifocus Image Fusion Based on Wavelet and Region Detection

This is a wavelet based region detection method that uses morphological operators and genetic algorithm (GA) during fusion process. Sharply focused regions from all images are selected using GA and combined to form fused image. The fusion algorithm is:

a. Wavelet Decomposition.

Apply wavelet Transform on both source images. If the size of source image is too small it loses actual detail. Using image of size 150 x 150 produces best result in region detection method.

b. Clear Pixel Distinguishing

The high frequency wavelet coefficients of the neighborhood of the pixel, in primary image and its blurred version created by applying Gaussian Smoothing kernel, are used to distinguishing the pixel quality. Pixel quality may be clear or blur. Pixel sharpness is analyzed by a threshold variable  $T$  whose value is determined by Genetic Algorithm (GA).

c. Sharply Focused Region Detection

Sharply focused regions are detected depending upon the pixel clarity. In multifocus images a complete object/region is in focus. Sharply focused pixels combined to form a sharply focused region. There may be some unresolved pixels in a region which are there due to noise. Morphological opening and closing operators are used to remove the additive and subtractive noisy pixels from these regions. Three binary regions are detected

- Focused in one image.
- Focused in 2<sup>nd</sup> image
- Either focused in both images or blurred in both images

d. Region Image Resizing

Binary region image's size is equal to size of the wavelet coefficients matrix that is less than the size of the original image. Binary region images are resized to original image size.

e. Reconstruction of The Fused Image

Finally the fused image is reconstructed using resized binary region images.

Select the clear pixel from corresponding source images otherwise take average.

Results are objectively evaluated using Root Mean Square Error (RMSE) and Gradient.

Results are compared with Haar wavelet and Morphological wavelet and found better.

This is a copy paste technique, so it may be very close to the original image. It gives better results in case of image misregistration/movement.

## **2.9 Image Fusion Algorithm Based on Neighbors and Cousins Information in Nonsubsampled Contourlet Transform Domain**

The proposed algorithm based on Contourlet transform is:

- a. Apply Nonsubsampled Contourlet Transform (NSCT) on registered source images.
- b. Get average of the approximate coefficients.
- c. Compute regional energy and correlation of cousins for each detailed coefficient.
- d. Calculate salience measure by multiplying regional energy and correlation of cousins.
- e. The detailed coefficients having higher value of salience measure is selected to be used for final image.
- f. Apply inverse NSCT to get resultant fused image.

Subjective as well as objective performance evaluation is performed using Mutual Information (MI) metric. The fusion results are compared with classical wavelet based and contourlet based techniques. The comparing results show that the proposed approach is better among these methods.

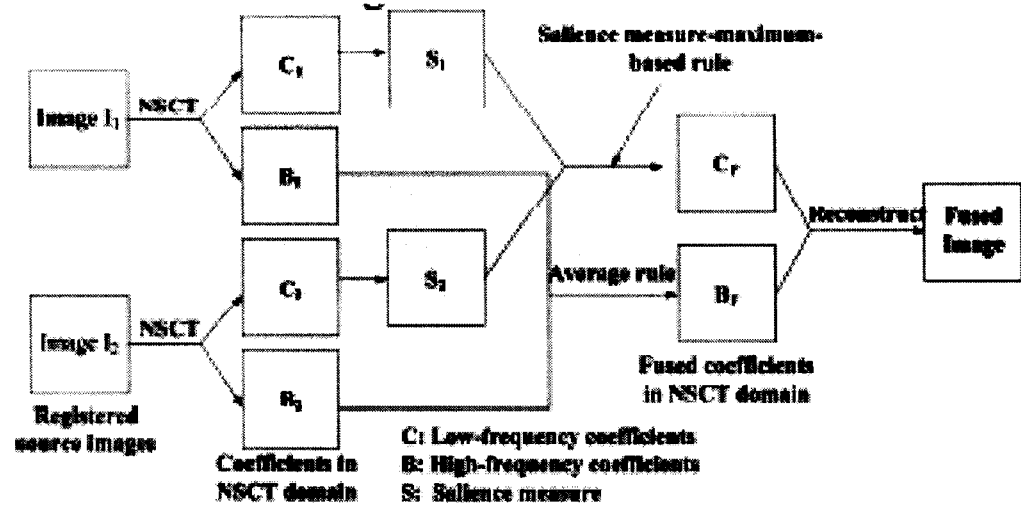


Figure 2-3: Image fusion using Nonsubsampled contourlet Transform

NSCT is a new technique. Different other methods of detailed coefficient selection can be explored.

### 3 Proposed Solution

Image fusion generates a fused image which is sharply focused and contains more information than all input images of the scene captured from multiple sensors simultaneously or at different times. When a camera needs to capture a scene that contains different objects at different depths, camera can't focus all objects at same time. So multiple images of the same scene are taken each having focus on different objects and then these images are fused to obtain an image in which all the objects are focused. To fulfill this purpose a fusion method is proposed which detects focused regions by detecting sharp edges using wavelet transform, edge detectors and morphological operations.

#### 3.1 Problem Statement

Literature survey depicts that a fair amount of work is done in image fusion and different approaches have been proposed with different pros and cons.

1. The average method produces blocking effects easily in the regions where the multi-focus images are significantly different.
2. Pyramid-based decomposition is a multiscale or multiresolution transform, but its decomposition coefficients are correlative, redundant and the amount of which is  $1/3$  more than original.
3. DWT fusion methods lose edge information during decomposition and reconstruction. The process of reconstruction i.e. IDWT, often leads to ringing effect in the fused image.

Fusion can be done both in spatial and transform domains. The spatial domain fusion methods produce good results when input images are in good condition but if there are complex details in images these methods are failed to produce good results. The challenge is to devise and implement an efficient image fusion algorithm, for microscopic and multifocus images, that provides better fusion results as compared to the existing algorithms.

## 3.2 Proposed Solution

In image fusion different objects and focused regions are main point of concern rather than individual pixels. As in multifocus images an object or a whole region is in focus in one image and some other object or region is in focus in other image. So instead of selecting pixel by pixel it is better to opt for block by block approach. The pixel by pixel approach produces a lot of salt and pepper noise which needs to be removed using different filters.

Proposed algorithm mainly focuses on wavelet based image fusion approach. Discrete wavelet transform is used for fusion due to the following reasons:

- It is a multiscale and multiresolution approach well suited to manage the different image resolutions. In recent years, some researchers [19–22] have studied multiscale representation (pyramid decomposition) of a signal and have established that multiscale information can be useful in a number of image processing applications including the image fusion.
- The discrete wavelets transform (DWT) allows the image decomposition in different kinds of coefficients preserving the image information. Such coefficients coming from different images can be appropriately combined to obtain new coefficients, so that the information in the original images is collected appropriately.
- Wavelet transform has resolution both in time field and frequency field. It can focus onto any details of the analyzed object by taking more and more fine step of time field or space field.

### 3.2.1 Proposed Block Level Multi-Focus Image Fusion Algorithms

The proposed scheme uses iterative technique. A basic algorithm is devised and then enhancements are made in it. Multilevel blocks are used in this technique. In proposed scheme blocks are of two types: blocks which lie on the boundary, here boundary means boundary of sharp and blur region, are called boundary blocks and non boundary blocks. Clarity of each block is checked using *Block Clarity Algorithm*. Copy paste technique is



used, i.e. fused image is generated by copying the clear non boundary blocks from source images and pasting in fused image. While *Boundary Block Fusion Algorithm* is used to fuse boundary blocks. Different proposed fusion algorithms are described below:

### a. Block Clarity Algorithm

- I. Discrete wavelet transform is applied to obtain the wavelet coefficients of the source blocks X and Y, each of size (p, p).
- II. Detailed wavelet coefficients  $xW_{\text{detail}}(m, n)$  and  $yW_{\text{detail}}(m, n)$  at level 1, for source blocks X and Y respectively, are computed; where *detail = horizontal, vertical and diagonal*.
- III. Local gradient of each detailed wavelet coefficient is computed as follows:

$$G(W_{\text{detail}}(m, n)) = \max \{ \text{mask}_i * W_{\text{detail}}(m, n) \mid i = 1 - 8 \}$$

Where the eight masks are given below:

|    |   |    |    |    |    |    |    |    |    |    |    |
|----|---|----|----|----|----|----|----|----|----|----|----|
| -1 | 0 | 1  | 0  | 1  | 1  | 1  | 1  | 1  | 1  | 1  | 0  |
| -1 | 0 | 1  | -1 | 0  | 1  | 0  | 0  | 0  | 1  | 0  | -1 |
| -1 | 0 | 1  | -1 | -1 | 0  | -1 | -1 | -1 | 0  | -1 | -1 |
| 1  | 0 | -1 | 0  | -1 | -1 | -1 | -1 | -1 | -1 | -1 | 0  |
| 1  | 0 | -1 | 1  | 0  | -1 | 0  | 0  | 0  | -1 | 0  | 1  |
| 1  | 0 | -1 | 1  | 1  | 0  | 1  | 1  | 1  | 0  | 1  | 1  |

- IV. Activity level of each wavelet coefficient is computed as follows:

$$A(W_{\text{detail}}(m, n)) = |W_{\text{detail}}(m, n)| + G(W_{\text{detail}}(m, n))$$

Where  $A(W_{\text{detail}}(m, n))$  reflects the activity level information of the wavelet coefficient  $W_{\text{detail}}(m, n)$ .

V. Block clarity level BCL of each block is computed as follows:

$$BCL = \sum_{\text{detail}} A(W_{\text{detail}}(m, n))$$

VI. Block having high value of BCL is considered clearer.

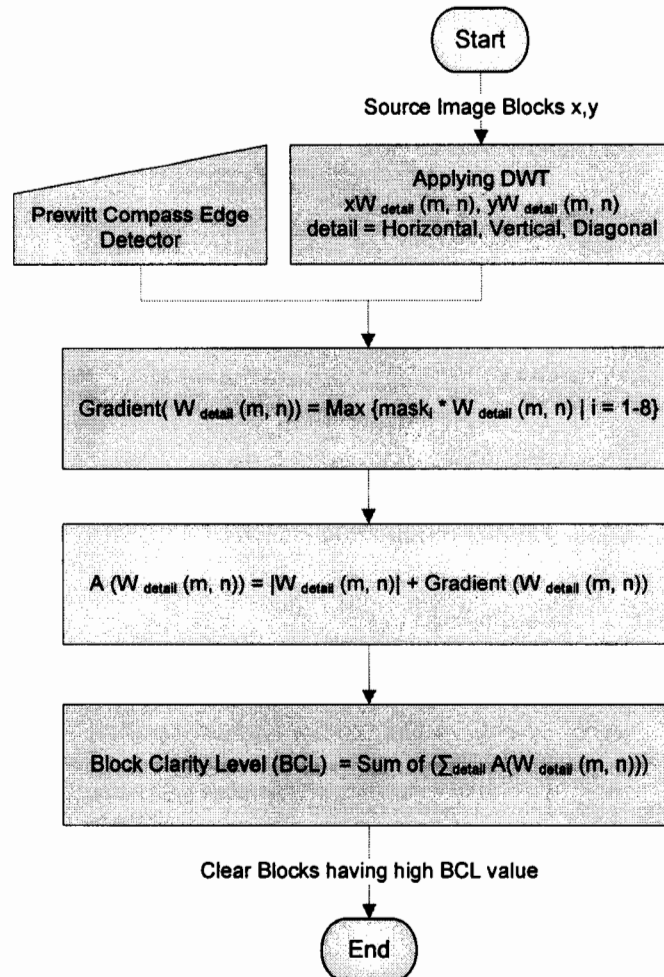


Figure 3-1: Block clarity algorithm

### b. Boundary Blocks Fusion Algorithm

- I. Discrete wavelet transform is applied to obtain the wavelet coefficients of the source blocks  $X$  and  $Y$ , each of size  $(p, p)$ .
- II. Wavelet coefficients  $xW_{coef}(m,n)$  and  $yW_{coef}(m,n)$  at level 5, for source blocks  $X$  and  $Y$  respectively, are computed; where *coef* means approximate, horizontal, vertical and diagonal.
- III. Obtain fused wavelet coefficients by averaging the approximate source coefficients and choosing maximum detailed (horizontal, vertical and diagonal) source coefficients
- IV. By applying inverse discrete wavelet transform on fused wavelet coefficients get fused boundary block

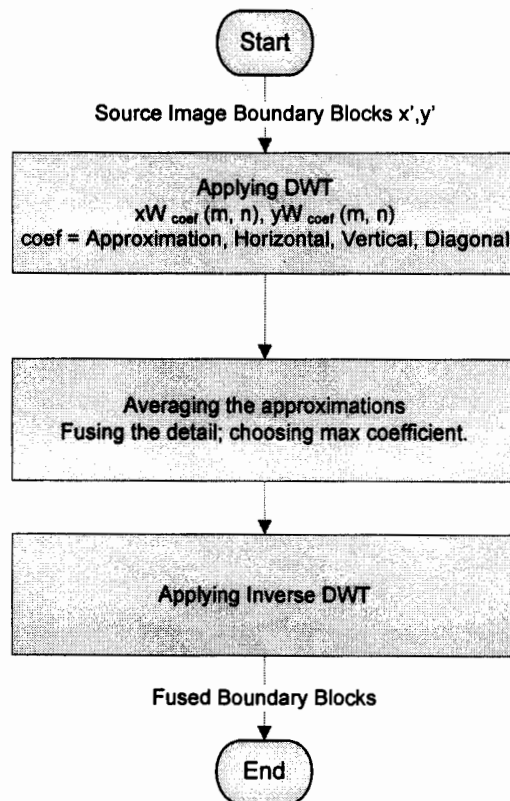


Figure 3-2: Boundary blocks fusion algorithm

### 3.2.1.1 Fusion using Single Level Blocks

In this technique input images are divided into blocks. Here blocks of size 16 x 16 are used. Block clarity is checked using *Block Clarity Algorithm*. Decision map (DM) for clear blocks from each image is constructed. *Boundary blocks* are detected from DM and fused with the help of *Boundary Block Fusion Algorithm*., whereas *non-boundary blocks* in DM are copied from the respective input images.

1. Divide the source images A and B into blocks of size  $P \times P$ .
2. Determine block clarity of every corresponding block of both images using *Block Clarity Algorithm*.
3. Construct decision map representing the clear blocks of both images.
4. Determine boundary blocks
5. Fuse boundary blocks using *Boundary Block Fusion Algorithm*
6. Copy non-boundary blocks as per decision map.
7. Merge boundary and non-boundary blocks to get final fused image

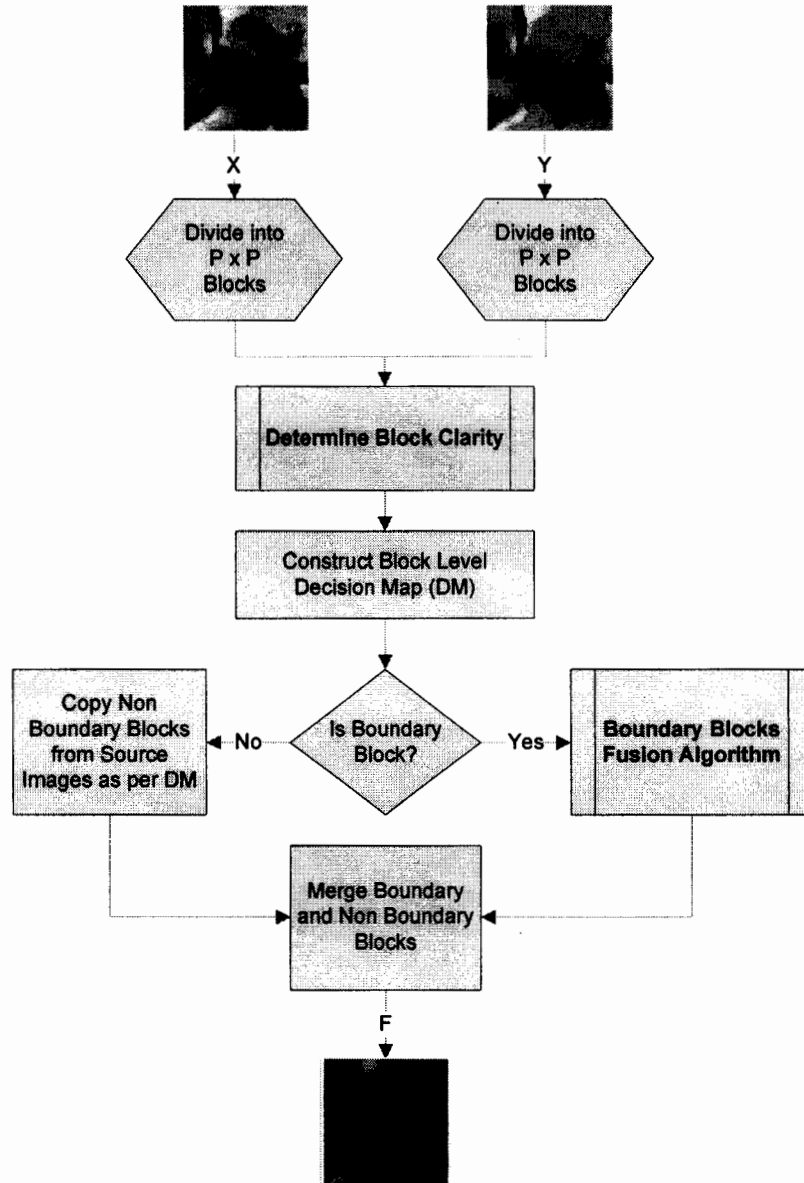


Figure 3-3: Fusion using Single level blocks

Algorithm is applied and tested for 16 x 16 and 8 x 8 blocks.

### 3.2.1.2 Fusion using Two Level Blocks

1. Divide the source images A and B into blocks of size  $P \times P$ . Here  $P = 16$
2. Determine block clarity of every corresponding block of both images using *Block Clarity Algorithm*.
3. Construct decision map representing the clear blocks of both images.
4. Determine boundary blocks
5. Divide boundary blocks into smaller blocks of size  $8 \times 8$ .
6. Determine block clarity of these new blocks using block clarity algorithm
7. Construct decision map for  $8 \times 8$  block size.
8. Determine boundary blocks again.
9. Fuse boundary blocks using *Boundary Block Fusion Algorithm*
10. Copy non-boundary blocks as per decision map.
11. Merge boundary and non-boundary blocks to get final fused image

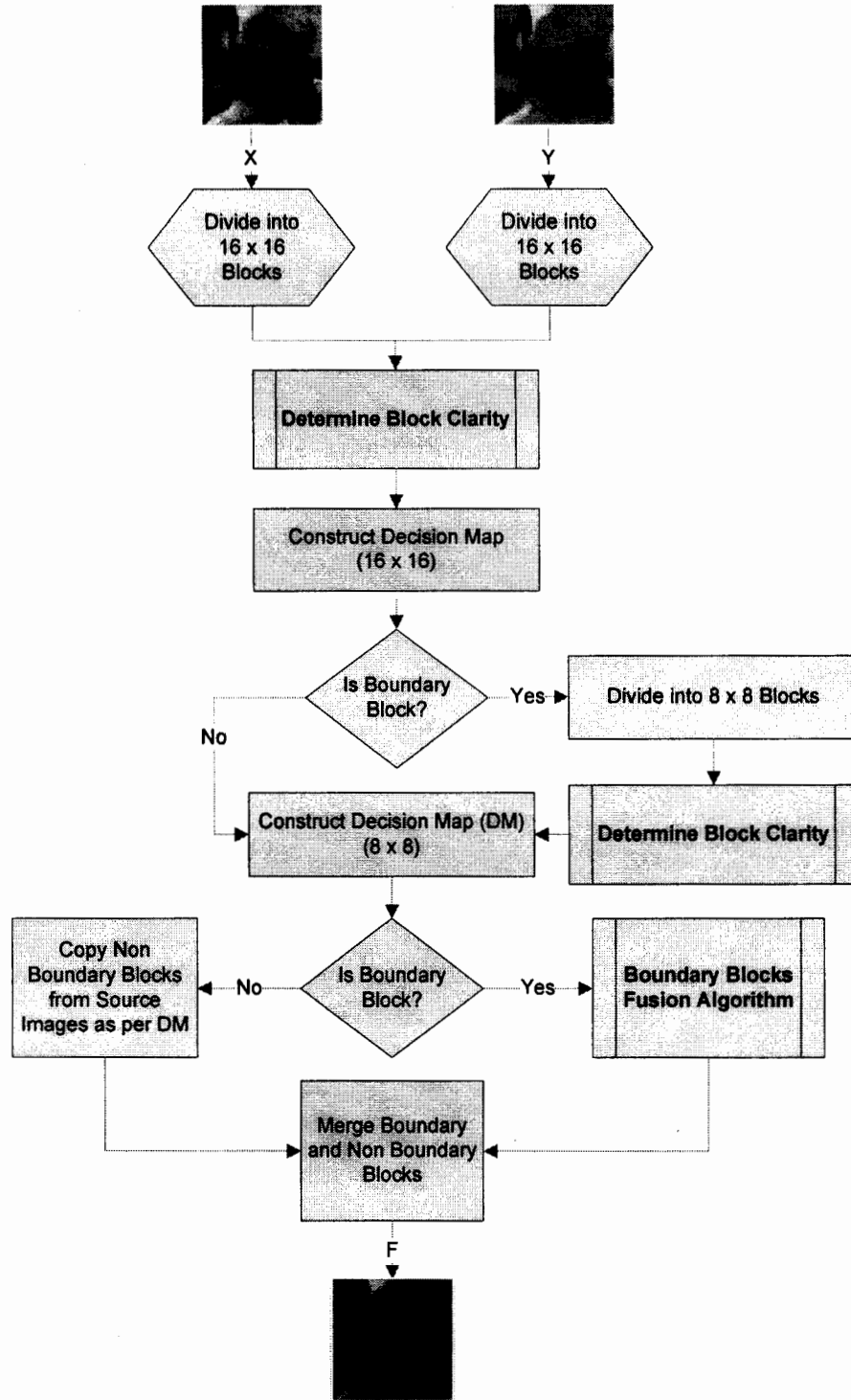


Figure 3-4: Fusion using Two Level Blocks

### 3.2.1.3 Fusion using Three Level Blocks

1. Divide the source images A and B into blocks of size  $P \times P$ . Here  $P = 16$
2. Determine block clarity of every corresponding block of both images using *Block Clarity Algorithm*.
3. Construct decision map representing the clear blocks of both images.
4. Determine boundary blocks.
5. Divide boundary blocks into smaller blocks of size  $8 \times 8$ .
6. Determine block clarity of these new blocks using block clarity algorithm
7. Construct decision map for  $8 \times 8$  block size.
8. Determine boundary blocks again.
9. Divide boundary blocks into smaller blocks of size  $4 \times 4$ .
10. Determine block clarity of these new blocks using block clarity algorithm
11. Construct decision map for  $4 \times 4$  block size.
12. Determine boundary blocks once again.
13. Fuse boundary blocks using *Boundary Block Fusion Algorithm*
14. Copy non-boundary blocks as per decision map.
15. Merge boundary and non-boundary blocks to get final fused image



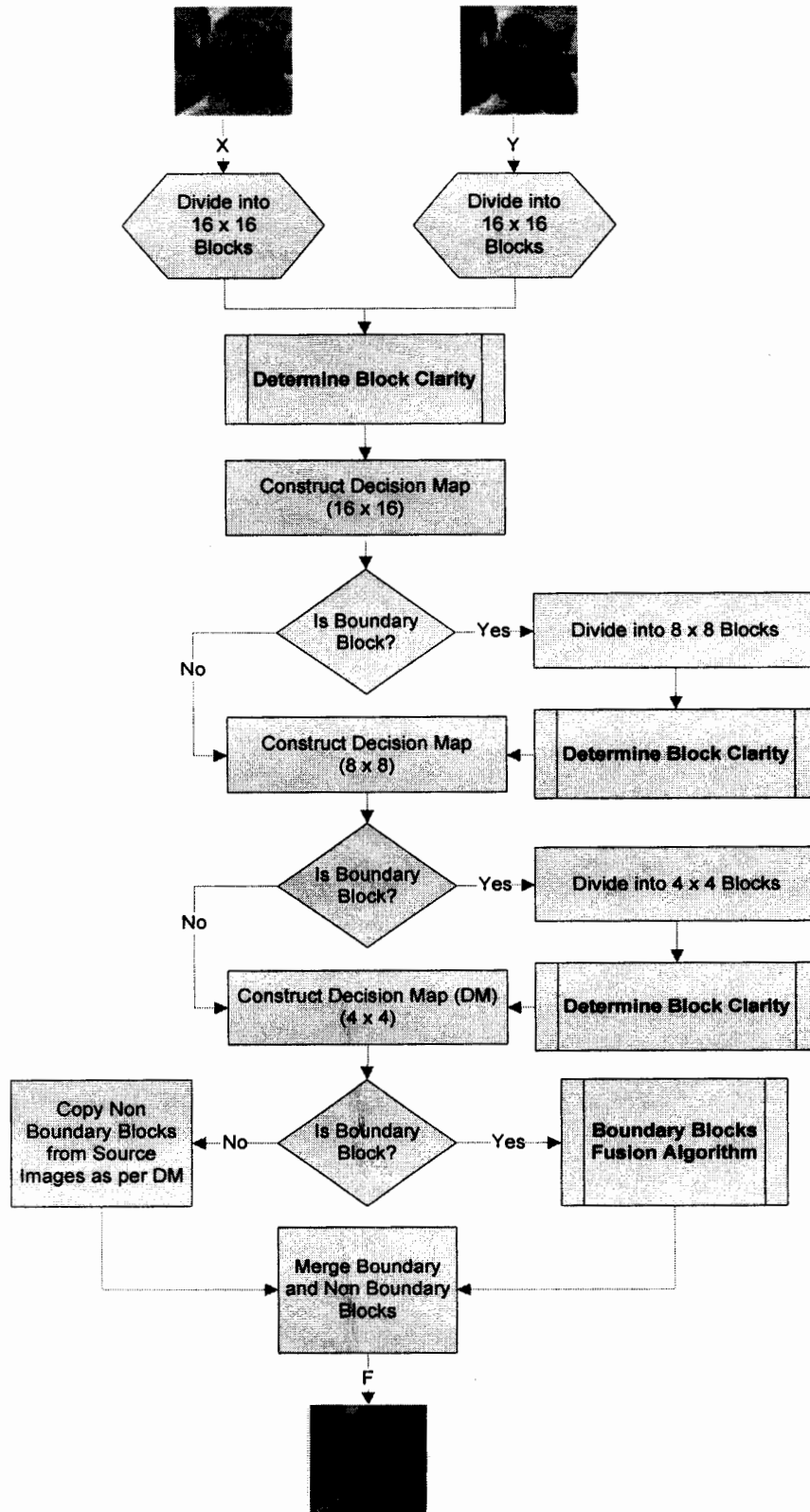


Figure 3-5: Fusion using Three Level Blocks

### 3.2.1.4 Fusion using Three Level Blocks and Mathematical Morphology

1. Divide the source images A and B into blocks of size  $P \times P$ . Here  $P = 16$
2. Determine block clarity of every corresponding block of both images using *Block Clarity Algorithm*.
3. Construct decision map representing the clear blocks of both images.
4. Determine boundary blocks.
5. Divide boundary blocks into smaller blocks of size  $8 \times 8$ .
6. Determine block clarity of these new blocks using block clarity algorithm
7. Construct decision map for  $8 \times 8$  block size.
8. Determine boundary blocks again.
9. Divide boundary blocks into smaller blocks of size  $4 \times 4$ .
10. Determine block clarity of these new blocks using block clarity algorithm
11. Construct decision map for  $4 \times 4$  block size.
12. Apply morphological close and open operations on the decision map.
13. Determine boundary blocks once again.
14. Fuse boundary blocks using *Boundary Block Fusion Algorithm*
15. Copy non-boundary blocks as per decision map.
16. Merge boundary and non-boundary blocks to get final fused image

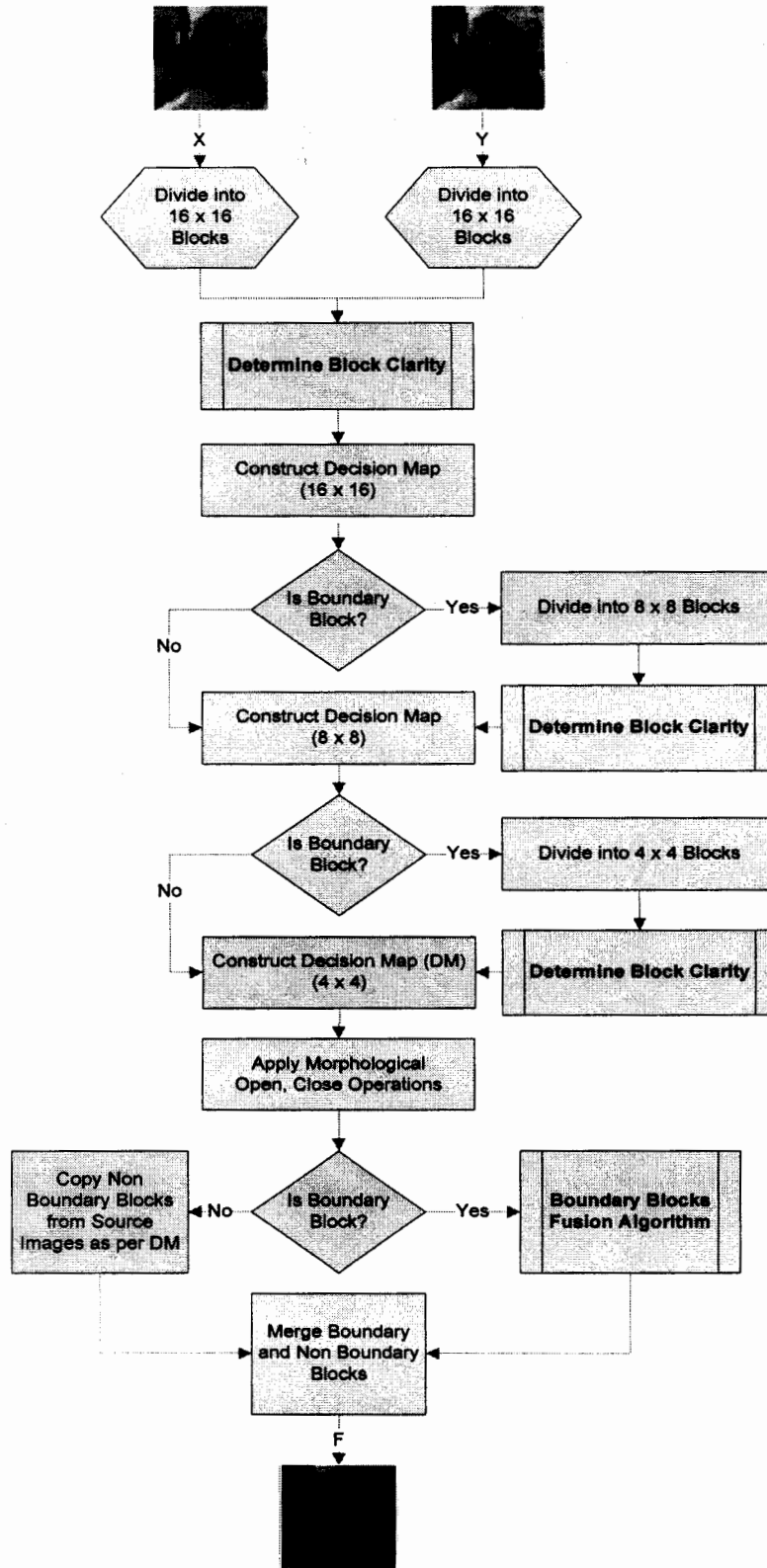


Figure 3-6: Fusion using Three Level Blocks and Mathematical Morphology

## 4 Implementation Detail

This chapter deals with implementation details of proposed approach. *MATLAB* has been chosen as a development tool because of the availability of required toolboxes and functions. The simulator is developed, compiled and tested in *MATLAB 7*.

### 4.1 Acquiring Image

Acquire a greyscale standard test image of size 512 x 512 to be processed for fusion process. Then using average filter mechanism, generate two multifocused images from it. Multifocused images can be of three different categories:

- a) Left and right multifocused
- b) Upper and lower multifocused
- c) Inner and outer multifocused

The Figure 4.2 shows all these three types of multifocused images for the original Barbara test image.



Figure 4-1: Original Barbara test image (512 x 512)

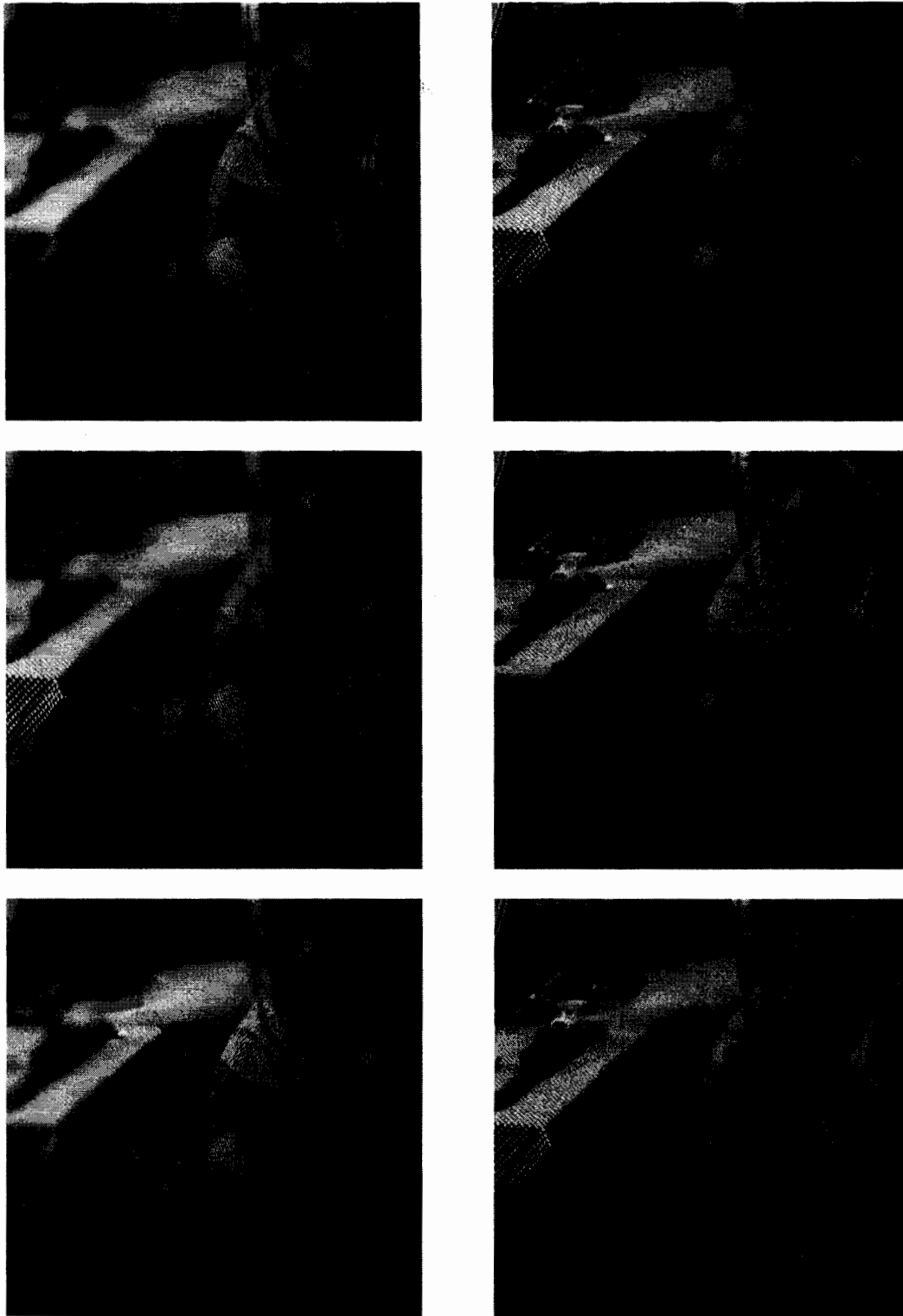


**Figure 4-2: Multifocused Sources Images of Barbara's**

## 4.2 Blocking and Discrete Wavelet Transform

Each image is divided into image blocks. It is an important step because all the further processing will be done on these image blocks not on the whole image. Block size is of basic importance. If blocks are of very large size then it may contain objects from focused or defocused areas. If blocks are of too small, it creates saw tooth function. In this research an adaptive block size is used. Block size is large if blocks is away from boundary and of small size when blocks are on boundary.

DWT is applied on every image block. For DWT, the wavelet basis “db4” at decomposition level one is used. DWT transforms or decomposes every input image block into an approximate and three details i.e., horizontal, vertical and diagonal details.

## 4.3 Maxima of Wavelet Coefficients using Compass Edge Detectors

Local gradients are actually an intermediate result for the calculation of activity levels of the wavelet coefficients. Gradients are mainly used in images for edge detection and extraction. Gradient represents a rapid change and since edges represents a rapid change in value, so at edges gradient value is high. *Compass Edge Detectors* are mainly used for edge detection. 8 kernels are convolved with detailed wavelet coefficients and a maximum of these 8 wavelet coefficients is computed using equation:

$$|G| = \max(|G_i| : i = 1 \text{ to } n)$$

Here  $G_i$  is the result of applying the kernel  $i$  on detailed wavelet coefficient and  $n$  represents number of kernels here value of  $n$  is 8. The maxima  $|G|$  represents the maximum value after applying these kernels. In proposed approach Prewitt edge detector is used. Two of its 8 kernels are shown in Figure 4.3. These gradient operators handle more gradual transition and noisier images better.

**Prewitt**

|    |   |   |
|----|---|---|
| -1 | 0 | 1 |
| -1 | 0 | 1 |
| -1 | 0 | 1 |

|    |    |   |
|----|----|---|
| 0  | 1  | 1 |
| -1 | 0  | 1 |
| -1 | -1 | 0 |

Figure 4-3: Prewitt Edge Detector

#### 4.4 Enhancement of Maxima

In the proposed approach, the effect of gradient is enhanced by adding the wavelet coefficients to its Maxima. As a result of this enhancement the edges become sharper and the detailed coefficients of focused objects increases. After the enhancement clear and focused blocks can be easily distinguished.

#### 4.5 Construction of Binary Decision Map

A binary Decision Map (DM) is constructed for the fused image. Decision map gives information about the clear blocks of different images. Block clarity is decided on the basis of the Block Clarity Level which is calculated by Block Clarity Algorithm. In adaptive block size technique a decision map is constructed for each block size giving information about the clear blocks for the resulting image. At first a decision map is constructed for 16 x 16 block size. From the DM boundary blocks are determined and further sub divided into small blocks (8 x 8). A new decision map is created for small blocks (8 x 8). Again from the DM boundary blocks are determined and further sub divided into further smaller blocks having size 4 x 4 and a new decision map is created for these blocks.

#### 4.6 Morphological Operations

The binary decision map obtained by comparing the enhanced values of wavelet coefficients represents the block needs to be copied from corresponding source images. But there is still some noise in it, a few white dots in black area means 1's in 0's area and black dots in white area i.e a few zero's in one's of the decision map. Thus binary decision map needs to be improved and morphological operations are used for improving the decision map.

Erosion and dilation are two essential morphological transformations. Dilation transformation is used to expand objects in an image and erosion reversely shrinks it. Erosion and dilation in different combinations give further transformations; two most significant of those are the morphological closing and morphological opening. Both closing and opening operations are used to smooth contour areas in an image. We use morphological close operation to fill white part, next the morphological open operation is used to fill black part.

#### 4.7 Construction of the fused image

A resulting image  $F(M, N)$  against the input images A and B, is constructed using the processed binary decision map  $BDM(M, N)$ . The blocks on boundary are fused using *Maximum Wavelet Coefficient Method* and block which are not on boundary are copied from the source images. The fused image obtained against left-focused and right-focused Barbara images is

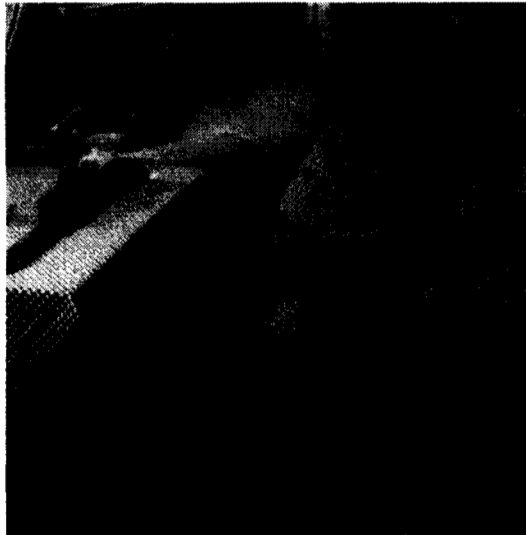


Figure 4-4: The resulting fused image

#### 4.8 The Simulation

The proposed approach is implemented and tested using *MATLAB*<sup>®</sup> 7.0. A simulation is prepared and the screen shot of the simulation is visible in Figure 4.7.



The foremost window of simulation allows user to select image, define multifocused option for image fusion process and Fusion Method. Three multifocusing options (left-right, upper-lower and inner-outer) are available here. Five Fusion Methods (16 by 16 Blocks, 8 by 8 Blocks, 2 Level Blocks, 3 Level Blocks and 3 Level Blocks with Morphology) are available here. User can select any image, exercise different focusing options using different Fusion Methods. The performance metrics i.e. Peak Signal to Noise Ratio (PSNR), Root Mean Square Error (RMSE) and Spatial Frequency (SF) at upper-right corner show the results obtained on selected image with selected multifocused option.

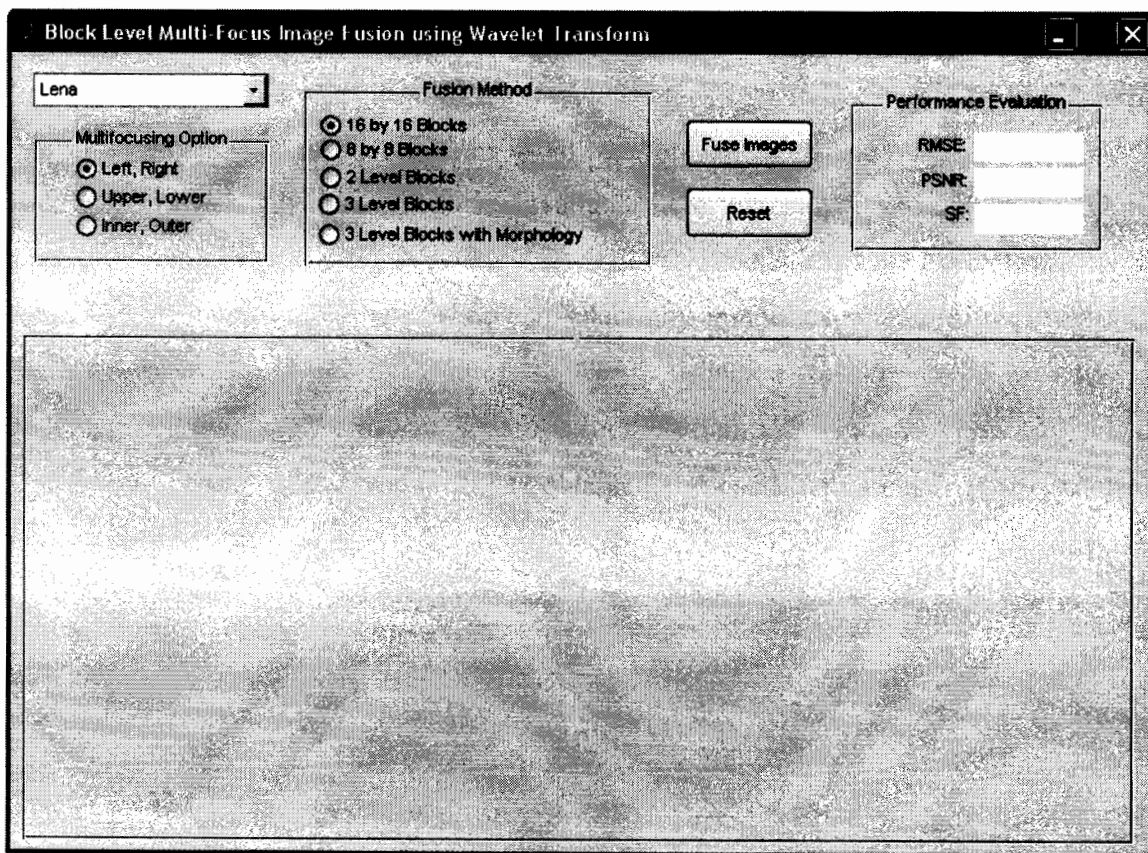


**Figure 4-5: Screen shot of start window in MATLAB**

Fineness of results after fusion process on selected standard images has been observed. Different standard test images have been taken and fusion results conducted on these a number of times to get high-quality image.

Different screen shots of the simulation exercising different available options are shown in Figure 4.8 to Figure 4.12.

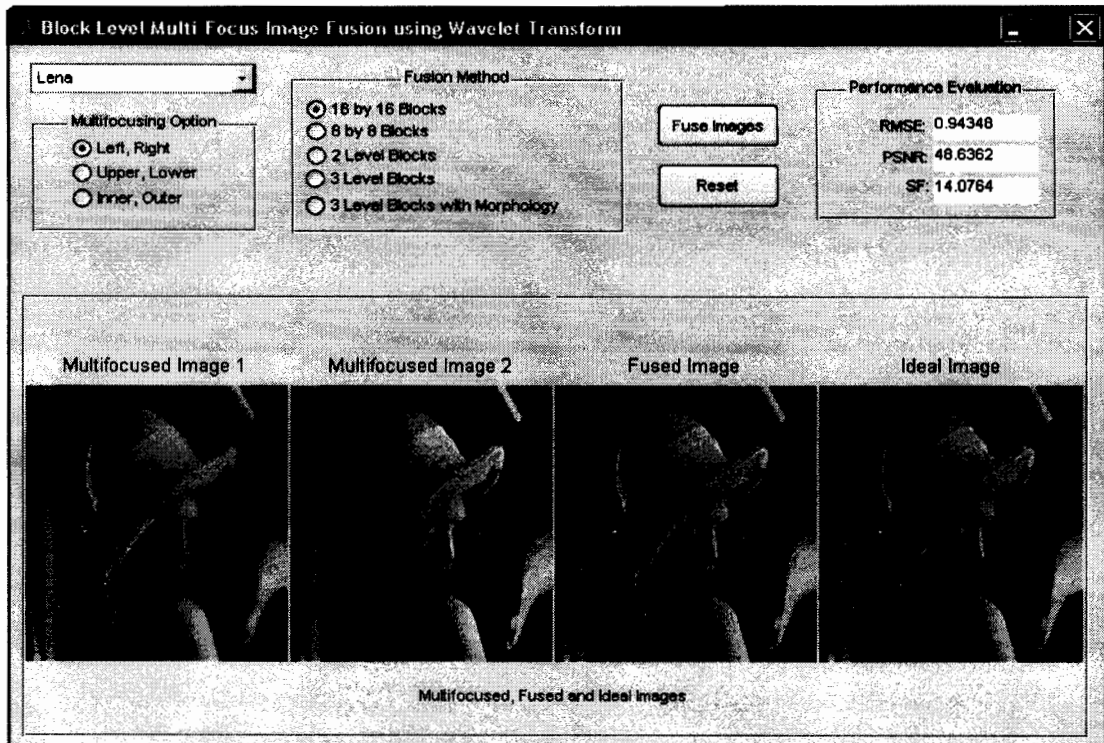


Figure 4-6: Fusion result against left-right defocused Lena image using 16 by 16 blocks

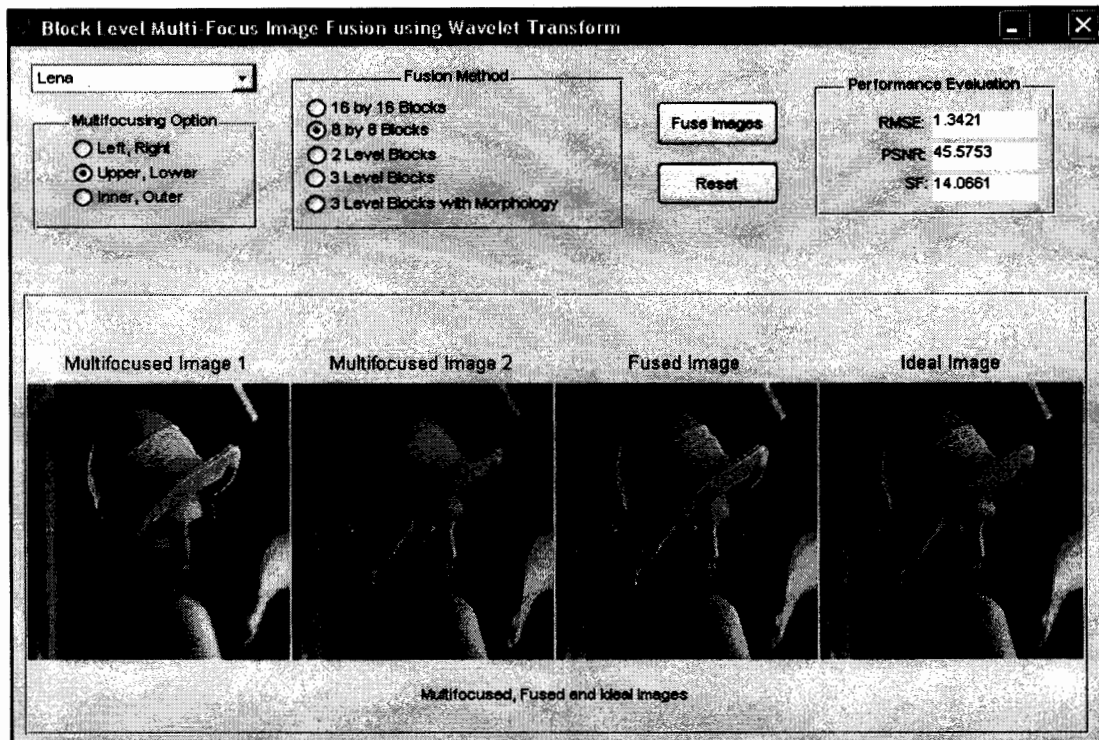


Figure 4-7: Fusion result against upper-lower defocused Lena image using 8 by 8 blocks

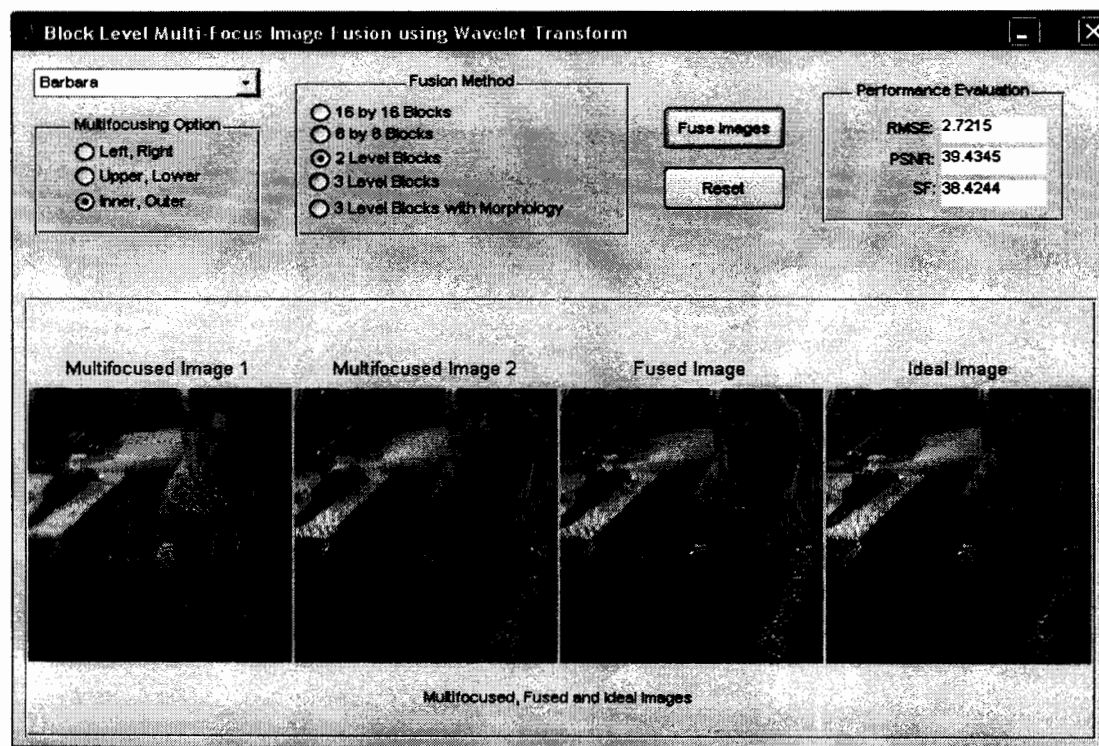


Figure 4-8: Result against inner-outer defocused Barbara image using 2-level blocks fusion method

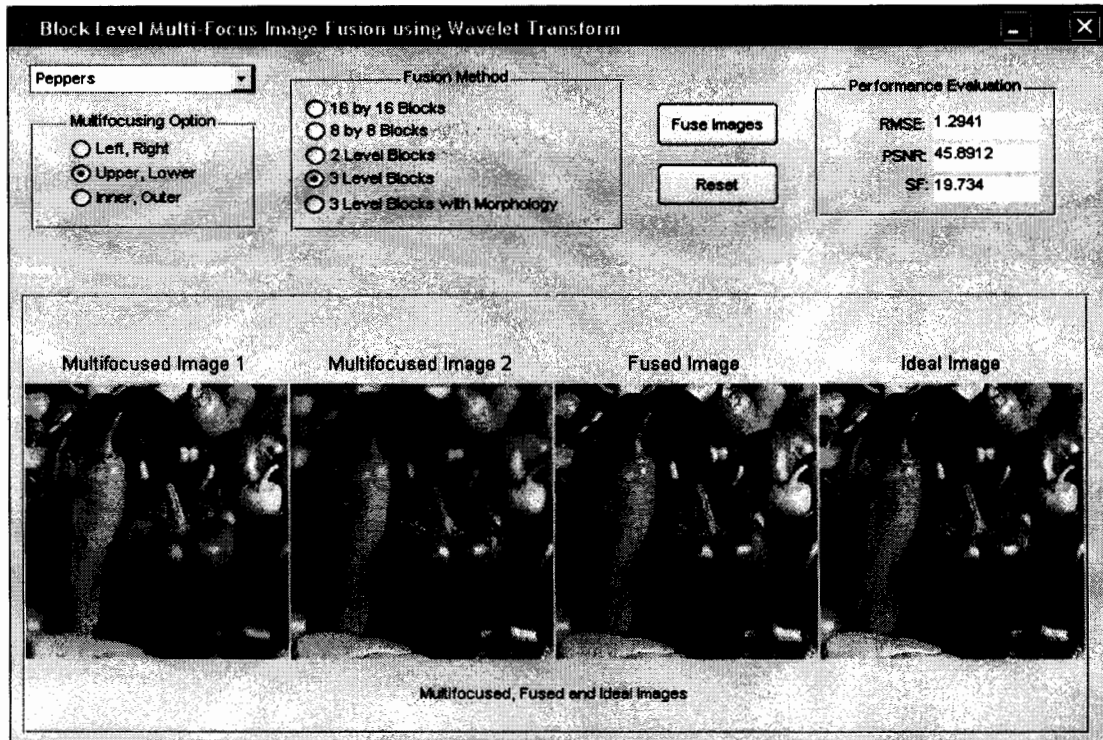


Figure 4-9: Result against upper-lower defocused Peppers image using 3-level blocks fusion method

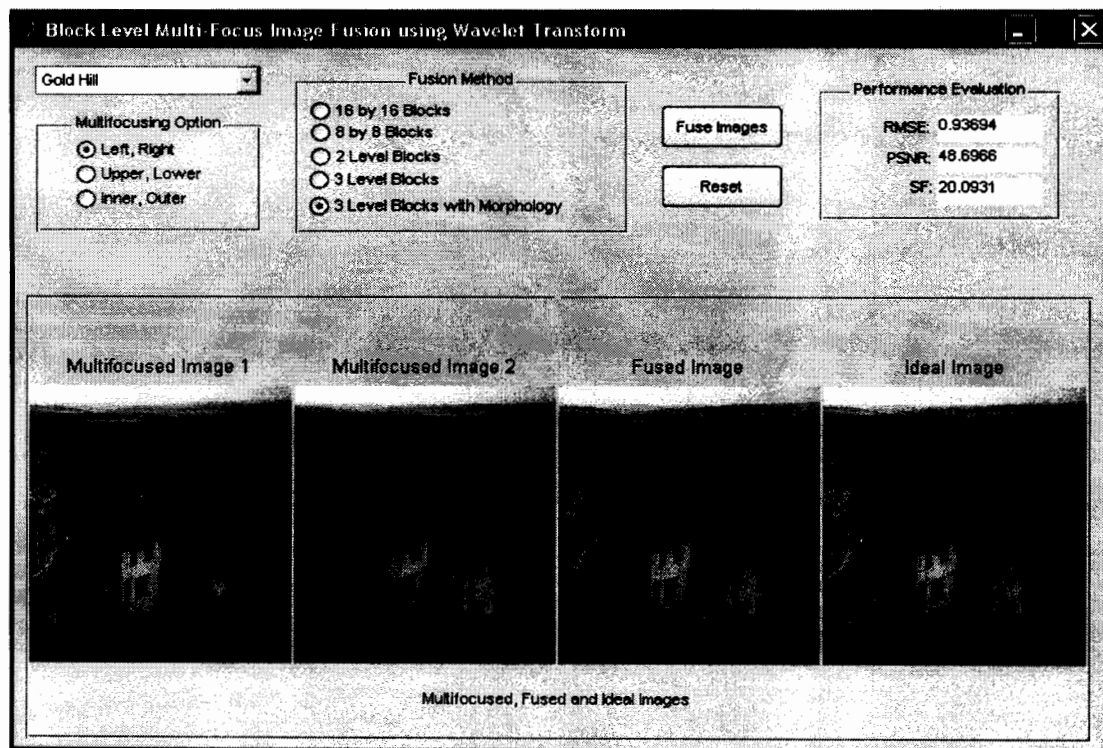


Figure 4-10: Result against left-right defocused Gold-Hill image using morphological method

## 5 Results and Comparisons

*MATLAB 7.0* is used to implement proposed method. Results are calculated on four standard grayscale images (i.e. Lena, Barbara, Hill and Peppers). Images are taken from World Wide Web. Each image is of size 512 x 512.

### 5.1 Image Quality Evaluation Matrices

The performance of fusion system can be measured by two types of metrics i.e. subjective and objective metrics. Following objective performance metrics have been analyzed to measure quality of reconstructed image.

- Peak Signal to Noise Ratio
- Root Mean Square Error
- Spatial Frequency

#### 5.1.1 Peak Signal to Noise Ratio (PSNR)

The quality of the fused image is measure by PSNR. More value of PSNR indicate better quality image. For two  $M \times N$  monochrome images  $O$  and  $F$ , where  $O$  is the referenced or ideal image and  $F$  is the fused or resultant image, it is defined as:

$$PSNR = 10 \cdot \log_{10} \left( \frac{\sum_{i=1}^M \sum_{j=1}^N 255^2}{\sum_{i=1}^M \sum_{j=1}^N [O(i, j) - F(i, j)]^2} \right).$$

#### 5.1.2 Root Mean Square Error (RMSE)

RMSE is the most valuable objective metric to compute the quality of the resultant images. Smaller value of RMSE indicate better quality image. RMSE is defined as:

$$RMSE = \sqrt{\frac{1}{M \times N} \sum_{i=1}^M \sum_{j=1}^N [O(i, j) - F(i, j)]^2}.$$

#### 5.1.3 Spatial Frequency (SF)

The higher the value of SF, the better is the quality. SF is defined as

$$SF = \sqrt{RF^2 + CF^2}$$

Where

$$RF = \sqrt{\frac{1}{M \times N} \sum_{i=1}^M \sum_{j=2}^N [\alpha(i, j) - F(i, j-1)]^2}$$

And

$$CF = \sqrt{\frac{1}{M \times N} \sum_{j=1}^N \sum_{i=2}^M [\alpha(i, j) - F(i-1, j)]^2}$$

## 5.2 Edge Detectors Comparison

The basic theme of this research depends upon the calculation of the maxima. Maxima is computed on the basis of gradient. Gradients are mainly used in images for edge detection and extraction. Various edge detectors, like Robinson, Sobel, Kirsch and Prewitt can be used for calculating local gradient. All these edge detectors are tested using *left-right focused Lena* image and it is found that *Prewitt Compass Edge Detector* produces the best results. Table 1, 2, 3, and 4 shows the results using Robinson, Sobel, Kirsch and Prewitt edge detectors respectively.

**Table 5-1: Fusion results using Robinson edge detector**

| Edge-Detector            |      |      |         |
|--------------------------|------|------|---------|
| Fusion Method            | RMSE | PSNR | SF      |
| 16 x 16                  |      |      | 10.9557 |
| 8 x 8                    |      |      | 10.9557 |
| 2 Levels                 |      |      | 10.9105 |
| 3 Levels                 |      |      | 10.9603 |
| 3 Levels with Morphology |      |      | 10.9619 |

**Table 5-2: Fusion results using Sobel edge detector**

| Edge Detector               | RMSE   | PSNR    | SF      |
|-----------------------------|--------|---------|---------|
| Fusion Method               |        |         |         |
| 16 x 16                     | 0.6712 | 50.9917 | 10.9576 |
| 8 x 8                       | 0.6712 | 50.9917 | 10.9577 |
| 2 Levels                    | 0.6712 | 50.9917 | 10.9589 |
| 3 Levels                    | 0.6712 | 50.9917 | 10.9595 |
| 3 Levels<br>with Morphology | 0.6712 | 50.9917 | 10.9574 |

Table 5-3: Fusion results using Kirsch edge detector

| Edge Detector               | RMSE   | PSNR    | SF      |
|-----------------------------|--------|---------|---------|
| Fusion Method               |        |         |         |
| 16 x 16                     | 0.7210 | 50.9601 | 10.9576 |
| 8 x 8                       | 0.7210 | 50.9601 | 10.9577 |
| 2 Levels                    | 0.7210 | 50.9601 | 10.9603 |
| 3 Levels                    | 0.7210 | 50.9601 | 10.9603 |
| 3 Levels<br>with Morphology | 0.7210 | 50.9601 | 10.9603 |

Table 5-4: Fusion results using Prewitt edge detector

| Edge Detector               | RMSE   | PSNR    | SF      |
|-----------------------------|--------|---------|---------|
| Fusion Method               |        |         |         |
| 16 x 16                     | 0.7210 | 50.9601 | 10.9576 |
| 8 x 8                       | 0.7210 | 50.9601 | 10.9577 |
| 2 Levels                    | 0.7210 | 50.9601 | 10.9603 |
| 3 Levels                    | 0.7210 | 50.9601 | 10.9603 |
| 3 Levels<br>with Morphology | 0.7210 | 50.9601 | 10.9603 |

### 5.3 Comparisons of Fused Image with Source Images

Tables 5.5, 5.6, 5.7, 5.8 and 5.9 show the comparisons of fused image and input images of Lena, Peppers, Barbara Gold Hill and Lab respectively. It becomes obvious after observing results from these tables that fusion process improves the image quality as the RMSE value of fused image is always small whereas PSNR and SF values are larger than that of the input images.

**Table 5-5: Comparison with Input Images of Lena**

| Multi-Input Region | RMSE          |               |               |               |               |                |               |               |                |
|--------------------|---------------|---------------|---------------|---------------|---------------|----------------|---------------|---------------|----------------|
|                    | Input Image 1 | Input Image 2 | Fused Image   | Input Image 1 | Input Image 2 | Fused Image    | Input Image 1 | Input Image 2 | Fused Image    |
| Left-Right         | 8.0112        | 9.0023        | <b>0.4107</b> | 30.0568       | 29.0438       | <b>55.8609</b> | 11.6337       | 8.6780        | <b>10.9619</b> |
| Upper-Lower        | 9.5939        | 7.2783        | <b>0.6564</b> | 28.4909       | 30.8903       | <b>51.7875</b> | 8.8707        | 11.4946       | <b>10.9572</b> |
| Inner-Outer        | 9.1557        | 7.7442        | <b>1.0181</b> | 28.8970       | 30.3512       | <b>47.9747</b> | 9.6621        | 10.8498       | <b>10.9433</b> |

**Table 5-6: Comparison with Input Images of Barbara**

| Multi-Input Region | RMSE          |                |             |               |               |                |               |               |                |
|--------------------|---------------|----------------|-------------|---------------|---------------|----------------|---------------|---------------|----------------|
|                    | Input Image 1 | Input Image 2  | Fused Image | Input Image 1 | Input Image 2 | Fused Image    | Input Image 1 | Input Image 2 | Fused Image    |
| Left-Right         | 17.2554       | <b>12.3477</b> | 0.4589      | 23.3923       | 26.2990       | <b>54.8958</b> | 15.4037       | 35.6866       | <b>29.4529</b> |
| Upper-Lower        | 16.0392       | <b>13.8631</b> | 0.7433      | 24.0271       | 25.2936       | <b>50.7076</b> | 20.0680       | 33.3080       | <b>29.4481</b> |
| Inner-Outer        | 18.7463       | <b>9.8957</b>  | 2.1556      | 22.6725       | 28.2219       | <b>41.4594</b> | 19.5587       | 33.5898       | <b>29.3236</b> |



Table 5-7: Comparison with Input Images of Peppers

| Multiscale Region | RMSE          |               |               |               |               |                |               |               |                |
|-------------------|---------------|---------------|---------------|---------------|---------------|----------------|---------------|---------------|----------------|
|                   | Input Image 1 | Input Image 2 | Input Image 3 | Input Image 4 | Input Image 5 | Input Image 6  | Input Image 7 | Input Image 8 | Input Image 9  |
| Left-Right        | 11.8229       | 11.7744       | <b>0.76</b>   | 26.6763       | 26.7120       | <b>50.5151</b> | 14.5612       | 14.2275       | <b>15.987</b>  |
| Upper-Lower       | 10.7791       | 12.7270       | <b>0.745</b>  | 27.4791       | 26.0363       | <b>50.6877</b> | 15.0254       | 13.7355       | <b>15.991</b>  |
| Inner-Outer       | 14.7310       | 7.9590        | <b>1.3818</b> | 24.7662       | 30.1136       | <b>45.3222</b> | 10.2825       | 17.5495       | <b>15.9659</b> |

Table 5-8: Comparison with Input Images of Gold Hill

| Multiscale Region | RMSE          |               |               |               |               |                |               |               |                |
|-------------------|---------------|---------------|---------------|---------------|---------------|----------------|---------------|---------------|----------------|
|                   | Input Image 1 | Input Image 2 | Input Image 3 | Input Image 4 | Input Image 5 | Input Image 6  | Input Image 7 | Input Image 8 | Input Image 9  |
| Left-Right        | 9.6669        | 11.6977       | <b>0.6406</b> | 28.4250       | 26.7688       | <b>51.9988</b> | 15.8672       | 12.7593       | <b>16.256</b>  |
| Upper-Lower       | 12.1303       | 9.1488        | <b>0.5784</b> | 26.4534       | 28.9035       | <b>52.887</b>  | 11.8019       | 16.5865       | <b>16.249</b>  |
| Inner-Outer       | 12.4965       | 8.5396        | <b>1.5295</b> | 26.1951       | 29.5020       | <b>44.4396</b> | 12.0070       | 16.4610       | <b>16.1962</b> |

#### 5.4 Comparison of Proposed Approaches with Existing Methods

Table 5.9 to Table 5.12 show the comparisons among the proposed approaches with DWT-I, DWT-II and the methods described in [30-34]. For DWT-based fusion schemes, the wavelet basis “db4” is used. The wavelet decomposition levels of DWT-I and DWT-II are six and five respectively. Consistency verification in a 3x3 window is only used for the DWT-II. The corresponding authors provide results of the schemes in [30-34].

Table 5-9: Image Fusion Methods' Comparisons for Lena Image

| Multifocus Regions | Left and Right |         |         | Upper and Lower |         |         |        |         |         |    |
|--------------------|----------------|---------|---------|-----------------|---------|---------|--------|---------|---------|----|
|                    | Fusion Method  | RMSE    | PSNR    | SF              | RMSE    | PSNR    | SF     | RMSE    | PSNR    | SF |
| DWT-I              | 1.2983         | 45.8631 | 14.0698 | 1.4912          | 44.6603 | 14.0588 | 1.7996 | 43.0275 | 14.0434 |    |
| DWT-II             | 1.0285         | 47.8866 | 14.0731 | 1.4414          | 44.9552 | 14.0506 | 1.8714 | 42.6874 | 14.0104 |    |
| in [30]            | 1.3231         | 45.6991 | 14.0685 | 1.4927          | 44.6516 | 14.064  | 1.8198 | 42.9303 | 14.0392 |    |
| in [31]            | 3.683          | 36.8069 | 13.5204 | 3.8159          | 36.4988 | 13.3428 | 3.9098 | 36.2877 | 13.3605 |    |
| in [32]            | 5.4541         | 33.3963 | 12.6394 | 4.7532          | 34.591  | 13.1646 | 5.0688 | 34.0327 | 12.9851 |    |
| in [33]            | 1.1863         | 46.6466 | 14.0516 | 1.4524          | 44.8894 | 14.0236 | 1.4282 | 45.0348 | 14.0084 |    |
| in [34]            | 1.1643         | 46.8096 | 13.9916 | 1.2434          | 46.2388 | 13.9552 | 1.383  | 45.3141 | 13.9089 |    |
| Proposed           |                |         |         |                 |         |         |        |         |         |    |
| 16 x 16            | 0.6119         | 52.3976 | 10.9558 | 1.407           | 45.1612 | 10.9451 | 1.317  | 45.3141 | 10.9451 |    |
| 8 x 8              | 0.8376         | 49.6705 | 10.9558 | 1.303           | 45.4455 | 10.9465 | 1.317  | 45.3141 | 10.9465 |    |
| 2 Levels           | 0.4958         | 54.2246 | 10.9604 | 1.2155          | 46.4359 | 10.9494 | 1.317  | 45.3141 | 10.9494 |    |
| 3 Levels           | 0.44           | 55.2621 | 10.9608 | 1.182           | 46.4359 | 10.9514 | 1.317  | 45.3141 | 10.9514 |    |
| 3 Levels           |                |         |         |                 |         |         |        |         |         |    |
| with Morphology    | 0.4107         | 55.8609 | 10.9619 | 1.1652          | 46.4359 | 10.9572 | 1.317  | 45.3141 | 10.9572 |    |

Table 5-10: Image Fusion Methods' Comparisons for Barbara Image

| Multifocus Regions          | Left and Right |         |         | Reference |         |         | Fused Image |         |         |
|-----------------------------|----------------|---------|---------|-----------|---------|---------|-------------|---------|---------|
| Fusion Method               | RMSE           | PSNR    | SF      | RMSE      | PSNR    | SF      | RMSE        | PSNR    | SF      |
| DWT-I                       | 1.8389         | 42.8398 | 29.4333 | 2.0037    | 42.094  | 29.436  | 2.2532      | 41.0748 | 29.4051 |
| DWT-II                      | 1.3938         | 45.2469 | 29.4361 | 1.7583    | 43.2291 | 29.4259 | 2.3986      | 40.5317 | 29.3706 |
| in [30]                     | 1.7456         | 43.2919 | 29.441  | 1.8919    | 42.5928 | 29.4394 | 2.1307      | 41.5603 | 29.4241 |
| in [31]                     | 5.2466         | 33.7333 | 28.3492 | 5.3947    | 33.4914 | 28.4519 | 5.6808      | 33.0427 | 28.3034 |
| in [32]                     | 6.8454         | 31.4228 | 28.8119 | 7.9284    | 30.1471 | 28.1963 | 7.1027      | 31.1023 | 28.5374 |
| in [33]                     | 2.3989         | 40.5306 | 29.3835 | 2.4298    | 40.4194 | 29.3763 | 2.5784      | 39.9039 | 29.3368 |
| in [34]                     | 1.7834         | 43.1058 | 29.3594 | 1.8687    | 42.7001 | 29.3477 | 1.9951      | 42.1315 | 29.2656 |
| Proposed                    |                |         |         |           |         |         |             |         |         |
| 16 x 16                     | 1.0256         | 47.9115 | 29.4511 | 1.0052    | 48.1715 | 29.4415 | 1.0256      | 47.9115 | 29.4511 |
| 8 x 8                       | 0.8513         | 49.5292 | 29.4529 | 0.8201    | 49.7517 | 29.4476 | 0.8513      | 49.5292 | 29.4529 |
| 2 Levels                    | 0.7705         | 50.3956 | 29.4517 | 0.7482    | 50.7535 | 29.4495 | 0.7705      | 50.3956 | 29.4517 |
| 3 Levels                    | 0.6585         | 51.7595 | 29.4512 | 0.6303    | 52.0077 | 29.4467 | 0.6585      | 51.7595 | 29.4512 |
| 3 Levels<br>with Morphology | 0.4589         | 54.8958 | 29.4529 | 0.4459    | 55.7076 | 29.4481 | 0.4589      | 54.8958 | 29.4529 |

Table 5-11: Image Fusion Methods' Comparisons for Peppers Image

| Multifocus Regions          | Left and Right |         |         | Upper and Lower |         |         | Left and Right |         |         |
|-----------------------------|----------------|---------|---------|-----------------|---------|---------|----------------|---------|---------|
|                             | RMSE           | PSNR    | SF      | RMSE            | PSNR    | SF      | RMSE           | PSNR    | SF      |
| DWT-I                       | 2.024          | 42.0067 | 15.9618 | 2.093           | 41.7153 | 15.9609 | 2.3561         | 40.6871 | 15.9408 |
| DWT-II                      | 1.6673         | 43.6906 | 15.9702 | 1.7773          | 43.1358 | 15.9624 | 2.1582         | 41.449  | 15.9364 |
| in [30]                     | 2.1073         | 41.6563 | 15.9584 | 2.1442          | 41.5053 | 15.9576 | 2.3003         | 40.8952 | 15.9464 |
| in [31]                     | 5.7325         | 32.964  | 15.2661 | 5.7087          | 33      | 15.2792 | 5.6914         | 33.0265 | 15.1747 |
| in [32]                     | 7.1395         | 31.0574 | 14.4864 | 7.0215          | 31.2022 | 14.6844 | 6.3359         | 32.0947 | 15.2745 |
| in [33]                     | 5.4568         | 33.3921 | 14.8664 | 5.4703          | 33.3706 | 14.8659 | 5.5941         | 33.1762 | 14.8354 |
| in [34]                     | 1.8753         | 42.6694 | 15.8314 | 1.8649          | 42.7175 | 15.8313 | 1.9694         | 42.2442 | 15.8456 |
| Proposed                    |                |         |         |                 |         |         |                |         |         |
| 16 x 16                     | 0.8702         | 49.3389 | 15.9874 | 0.745           | 50.6057 | 15.9912 | 0.76           | 50.5151 | 15.987  |
| 8 x 8                       | 0.8575         | 49.4662 | 15.9872 | 0.8601          | 50.5133 | 15.9949 | 0.7601         | 50.5133 | 15.9869 |
| 2 Levels                    | 0.8575         | 49.4662 | 15.9872 | 0.8601          | 50.5133 | 15.9949 | 0.7601         | 50.5133 | 15.9869 |
| 3 Levels                    | 0.7601         | 50.5133 | 15.9869 | 0.745           | 50.6057 | 15.9912 | 0.76           | 50.5151 | 15.987  |
| 3 Levels<br>with Morphology | 0.76           | 50.5151 | 15.987  | 0.745           | 50.6057 | 15.9912 | 0.76           | 50.5151 | 15.987  |

Table 5-12: Image Fusion Methods' Comparisons for Gold-Hill Image

| Multifocus Regions          | Left and Right |         |         | Upper and Lower |         |         | Left and Right |         |         |
|-----------------------------|----------------|---------|---------|-----------------|---------|---------|----------------|---------|---------|
|                             | RMSE           | PSNR    | SF      | RMSE            | PSNR    | SF      | RMSE           | PSNR    | SF      |
| DWT-I                       | 1.5195         | 44.497  | 16.2341 | 1.4867          | 44.6863 | 16.23   | 1.777          | 43.1372 | 16.2287 |
| DWT-II                      | 1.2584         | 46.1344 | 16.2391 | 1.2877          | 45.9345 | 16.2296 | 1.8886         | 42.6082 | 16.2127 |
| in [30]                     | 1.5558         | 44.2917 | 16.2399 | 1.4736          | 44.7631 | 16.2374 | 1.7246         | 43.3971 | 16.2334 |
| in [31]                     | 4.3686         | 35.3239 | 15.7418 | 4.3668          | 35.3276 | 15.5824 | 4.5751         | 34.9228 | 15.5634 |
| in [32]                     | 6.2954         | 32.1504 | 15.2236 | 5.6175          | 33.14   | 15.4538 | 5.9288         | 32.6714 | 15.4395 |
| in [33]                     | 1.1953         | 46.5814 | 16.2176 | 1.3641          | 45.4341 | 16.2008 | 1.9861         | 42.1709 | 16.1566 |
| in [34]                     | 1.2487         | 46.2017 | 16.1644 | 1.2513          | 46.1839 | 16.1562 | 1.381          | 45.3271 | 16.1082 |
| Proposed                    |                |         |         |                 |         |         |                |         |         |
| 16 x 16                     | 0.9214         | 48.8417 | 16.2509 | 0.8002          | 50.0672 | 16.2491 | 0.8002         | 48.8417 | 16.2509 |
| 8 x 8                       | 0.7426         | 50.7154 | 16.2525 | 0.6406          | 52.1387 | 16.2491 | 0.6406         | 50.7154 | 16.2525 |
| 2 Levels                    | 0.7426         | 50.7154 | 16.2525 | 0.6406          | 52.1387 | 16.2491 | 0.6406         | 50.7154 | 16.2525 |
| 3 Levels                    | 0.6406         | 51.9988 | 16.256  | 0.5780          | 52.437  | 16.2491 | 0.5780         | 51.9988 | 16.256  |
| 3 Levels<br>with Morphology | 0.6406         | 51.9988 | 16.256  | 0.5780          | 52.437  | 16.2491 | 0.5780         | 51.9988 | 16.256  |

Figure 5.1 graphically demonstrates the comparisons of RMSE values of proposed method and the other methods by left right defocusing the input image. Similarly Figure 5.2 and Figure 5.3 present the comparisons among PSNR and SF values of these techniques.

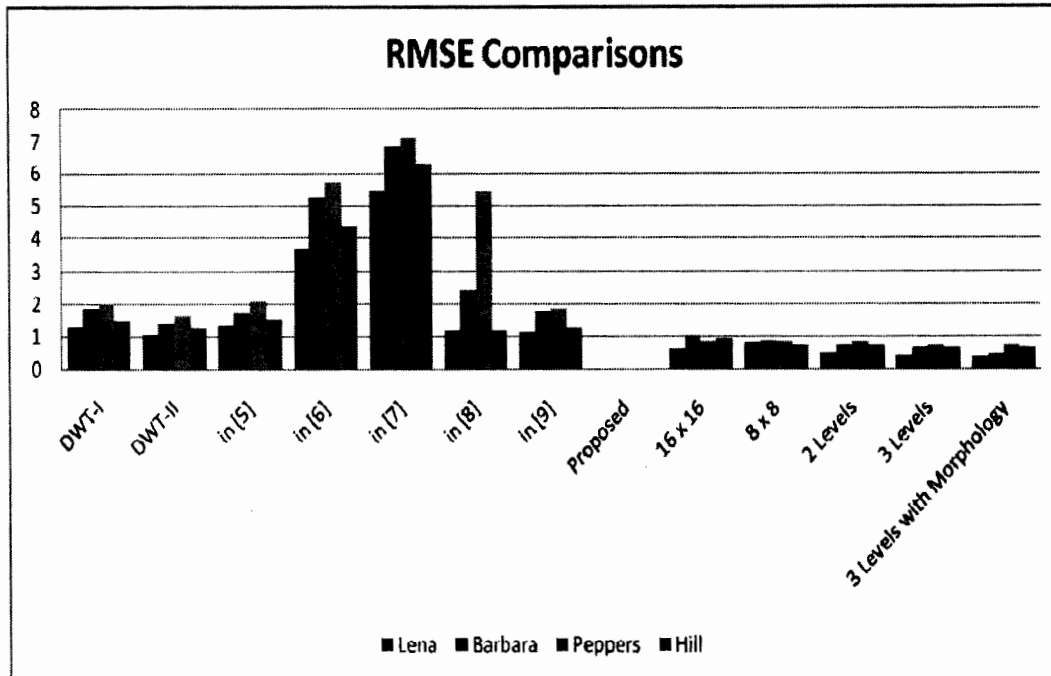


Figure 5-1: Graphical Comparison of RMSE

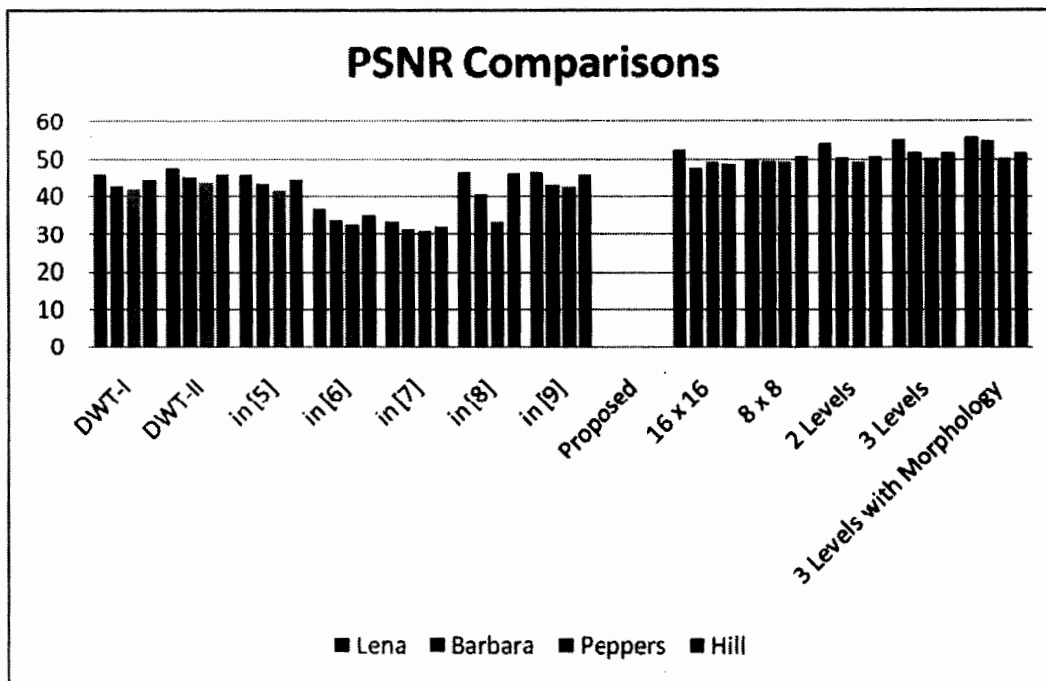


Figure 5-2: Graphical Comparison of PSNR

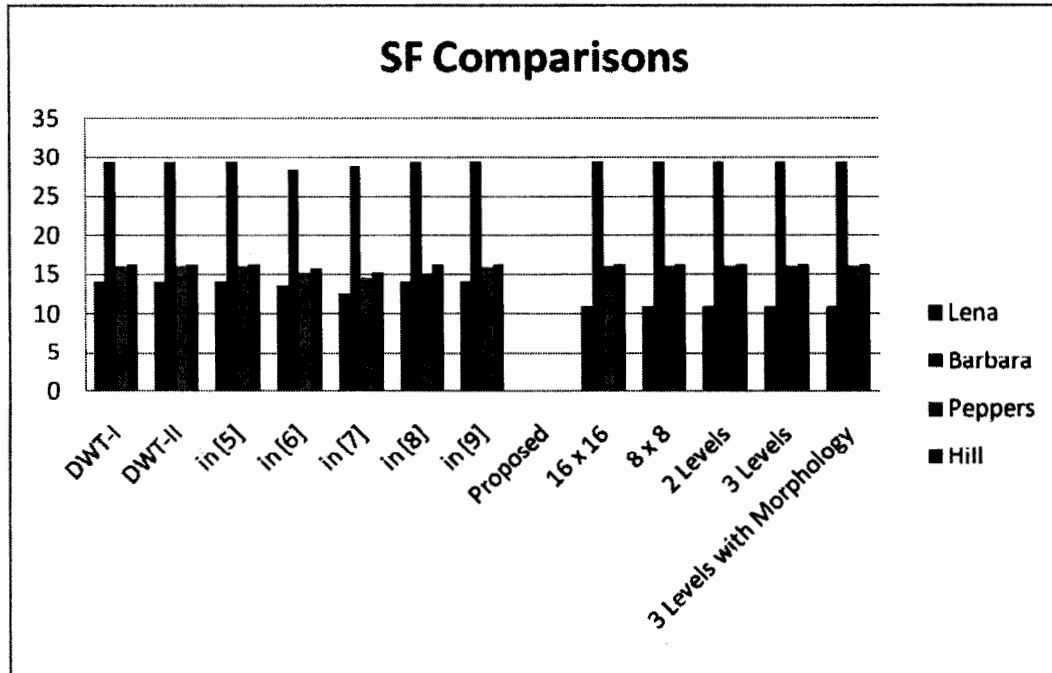


Figure 5-3: Graphical Comparison of SF

Results show that the proposed method has higher values of SF and PSNR, minimum value of RMSE. It means that proposed approach attained better performance than the above methods.

## 6 CONCLUSION AND FUTURE WORK

### 6.1 Conclusion

Image fusion has its applications in many fields such as computer vision, automatic object detection, robotics, remote sensing, military and law enforcement, medical imaging and manufacturing. The mixture of multiple source images of the same scene, from different sources, with the aim to obtain new or more precise knowledge about the scene, which is appropriate for computer perception and human vision, is called for image fusion. The fused image has all more useful information than any of the single input image and can describe the scene more appropriately. The fused image has less noise and inconsistencies.

In the past, multifocus image fusion has been carried out using a variety of techniques. All fusion techniques extract valuable information from all source images to create fused image containing all objects 'in focus'.

The proposed technique tries to combine decomposition based technique with other techniques to attain better results. It produces better results in comparisons with classical decomposition based fusion techniques as experimental results produced with proposed technique provides lower value of RMSE and higher value of PSNR than previous approaches. In this research a technique is proposed which is an integration of discrete wavelet transform, maxima and morphological operation. Fusion is done at image blocks not image pixels. Different experiments using different block sizes are carried out and different evaluation matrices RMSE, PSNR and SF are calculated. Results are compared with a number of previous researches. It was found that block level fusion produces much better results than pixel based fusion and an adaptive block size, on the basis of boundary of objects, produces the best fusion results.



## 6.2 Future Work

The future works for this research are to:

- Apply other latest transforms like curvelet other than wavelet transform
- Try some other technique to fuse boundary blocks
- Test and enhance the algorithm for more than two images and for colored image
- Modify and amend algorithm for images other than microscopic images.

## 7 References

- [1] Gonzalo Pajares, Jesus Manuel de la Cruz: A wavelet-based image fusion tutorial. *Pattern Recognition* 37 (2004) 1855–1872.
- [2] Gemma Piella: A region-based multiresolution image fusion algorithm. ISIF Fusion 2002 conference.
- [3] C. Y. Wen, J. K. Chen: Multi-resolution image fusion technique and its application to forensic science. *Forensic Science International* 140 (2004) 217–232.
- [4] Min Li, Wei Cai, Zheng Tan: A region-based multi-sensor image fusion scheme using pulse-coupled neural network. *Pattern Recognition Letters* 27 (2006) 1948–1956.
- [5] Zhiguo Jiang, Dongbing Han, Jin Chen, Xiaokuan Zhou: A wavelet based algorithm for multi-focus micro-image fusion. *Proceedings of the Third International Conference on Image and Graphics 2004*.
- [6] Z. Zhang, R.S. Blum, A categorization of multiscale decomposition-based image fusion schemes with a performance study for a digital camera application, *Proc. IEEE* 87 (8) (1999) 1315–1326.
- [7] T. Ranchin, L. Wald, Fusion of high spatial and spectral resolution images: the ARSIS concept and its implementation, *Photogramm. Eng. Remote Sensing* 66 (1) (2000) 49–61.
- [8] H. Li, B.S. Manjunath, S.K. Mitra, Multisensor image fusion using the wavelet transform, *Graphical Models Image Process.* 57 (3) (1995) 235–245
- [9] B. Garguet-Duport, J. Girel, J. Chassery, J.G. Pautou, The use of multiresolution analysis and wavelets transform for merging SPOT panchromatic and multispectral image data, *Photogramm. Eng. Remote Sensing* 62 (9) (1996) 1057–1066.
- [10] Shutao Li, James T Kwok and Yaonan Wang, “Multifocus image fusion using artificial neural networks” , *Pattern Recognition Letters*, Vol.23, pp. 985-997, 2002.

- [11] Shutao Li, James Tin-Yau Kwok, Ivor Wai-Hung Tsang and Yaonan Wang, "Fusing images with different focus using support vector machines", IEEE Transaction on Neural Networks, Vol. 15, pp. 1555-1561, 2004
- [12] Olivier Chapelle, Patrick Haffner and Vladimir N. Vapnik, "Support vector machines" for histogram-based image classification", IEEE Transactions on neural Networks, Vol.10, pp 1055-1064, 1999
- [13] Shutao Li and Yaonan Wang, "Multifocus image fusion using spatial features and support vector machine", ISNN 2005, LNCS 3497, Springer-verlag, Berlin Heidelberg, Germany, pp. 753-758, 2005
- [14] LI Guo-xin, WANG Guo-yu, WANG Ru-lin, and ZHANG Li, "Multi-focus Image Fusion Based on Automatic Focus algorithm", Application Research of Computers, vol. 22, no.3, pp.166-168,2005
- [15] WANG Hong, JING Zhong-liang, and LI Jian-xun, "Multi-focus Image Fusing Using Image Block Segment", Journal of shanghai Jiaotong University, vol. 37, pp. 1743-1746, 2003
- [16] CHU Heng, LI Jie and ZHU Weie, "A Novel Support Vector Machine-Based Multifocus Image Fusion Algorithm" IEEE 2006, pp 500-504
- [17] Yu Song, Mantian Li, Qingling Li and Lining Sun, "A New Wavelet Based Multi-focus Image Fusion Scheme and Its Application on Optical Microscopy" Proceeding of International Conference on Robotics and Bioimimetics, IEEE, pp 401-405, 2006
- [18] Yinghua Lu, Xue Feng, Jingbo Zhang, Rujuan Wang, Kaiyuan Zheng and Jun Kong "A Multi-focus Image Fusion Based on Wavelet and Region Detection" Proceedings of EUROCON: The International Conference on Computer as a Tool, pp 294-298, 2007
- [19] A. Rosendfeld, M. Thurston, Edge and curve detection for visual scene analysis, IEEE Trans. Comput. 20 (1971) 562-569
- [20] P.J. Burt, E. Adelson, The Laplacian pyramid as a compact image code, IEEE Trans. Commun. 31 (1983) 532-540.

- [21] E.H. Adelson, C.H. Anderson, J.R. Bergen, P.J. Burt, J. Ogden, Pyramid methods in image processing, *RCA Eng.* 29 (6) (1984) 33–41.
- [22] T. Lindeberg, *Scale-Space Theory in Computer Vision*, Kluwer, Norwell, MA, 1994.
- [23] Toet A. Hierarchical image fusion. *Machine Vision and Applications*. 3(1): Jan.,1990, 1-11
- [24] Toet A. Multiscale contrast enhancement with application to image fusion. *Optical Engineering*. 31(5): May, 1992, 1026-1031
- [25] Toet A. van hyven L J, Valeton J M. Merging thermal and visual images by a contrast pyramid. *Optical Engineering*. 28(7): July, 1989, 789-792,
- [26] Toet A. Image fusion by a ratio of low-pass pyramid. *Pattern Recognition Letters*. 9(4): April, 1989, 245-253
- [27] W.W Wang, P L Shui, G X Song Multifocus Image Fusion in Wavelet Domain. *IEEE, Machine Learning and Cybernetics*, Xi'an, Nov, 2003, 2887 – 2890
- [28] Gonzalez and Woods, “Digital Image Processing,” 3rd Edition, ISBN: 9780131687288, Prentice Hall, 2008
- [29] <http://homepages.inf.ed.ac.uk/rbf/HIPR2/matmorph.htm>
- [30] C. Hua-Wen and L. Shu-Duo, “Image fusion based on addition of wavelet coefficients,” in *International Conference on Wavelet Analysis and Pattern Recognition*, Vol. 4, 2007, pp. 1585 – 1588.
- [31] Lei Tang and Zong-gui Zhao, “The Wavelet-based Contourlet Transform for Image Fusion,” in the *Eighth ACIS International Conference on Software Engineering, Artificial Intelligence, Networking, and Parallel/Distributed Computing*, Vol. 2, 2007, pp. 59 – 64.
- [32] Muwei Jian, Junyu Dong and Yang Zhang, “Image Fusion Based on Wavelet Transform,” in the *Eighth ACIS International Conference on Software Engineering, Artificial Intelligence, Networking, and Parallel/Distributed Computing*, Vol. 1, 2007, pp. 713 – 718.
- [33] Qu Xiaobo and Yan Jingwen, “Image Fusion Algorithm Based on Features Motivated Multi-Channel Pulse Coupled Neural Networks,” in the 2nd

International Conference on Bioinformatics and Biomedical Engineering, 2008, pp. 2103 – 2106.

- [34] Xiao-Bo Qu, Guo-Fu Xie, Jing-Wen Yan, Zi-Qian Zhu and Ben-Gang Chen, “Image fusion algorithm based on neighbors and cousins information in nonsubsampling contourlet transform domain,” in International Conference on Wavelet Analysis and Pattern Recognition, Vol. 4, 2007, pp. 1797 – 1802.

